From the Department of Clinical Neuroscience and
the Center for Hearing and Communication Research,
Karolinska Institutet, Stockholm, Sweden

CHARACTERIZATION OF COCHLEAR DEGENERATION IN THE INNER EAR OF THE GERMAN WALTZING GUINEA PIG: A MORPHOLOGICAL, CELLULAR, AND MOLECULAR STUDY

Zhe Jin

Stockholm 2006

Published and printed by Karolinska University Press
Box 200, SE-171 77 Stockholm, Sweden

ISBN 91-7140-971-8

To my beloved family

ABSTRACT

The German waltzing guinea pig is a new strain of animals with yet unknown gene mutation(s) displaying recessively inherited cochleovestibular impairment. The homozygous animals (*gw/gw*) are deaf already at birth and display typical waltzing behavior throughout life. The heterozygous animals (*gw/+*) do not suffer from hearing loss and vestibular symptoms. The present thesis is focused on the homozygous German waltzing guinea pig (*gw/gw*) and its cochlear deficits.

Cochlear histological analysis in the postnatal animals revealed a characteristic cochleosaccular defect: collapse of scala media compartment, atrophy of stria vascularis, degeneration of sensory hair cells, and slow loss of spiral ganglion neurons. The stria vascularis was atrophic and appeared as a single layer composed of only marginal cells, as further evidenced by morphometric measurement of strial height and width. The abnormally appearing strial intermediate cells (melanocytes) were sparsely scattered in the spiral ligament, whereas strial basal cells were difficult to identify. The degree of sensory hair cell degeneration varied even among animals of the same age. Morphometric analysis of the spiral ganglion neuron profile density showed a significant reduction in the old (1-2 years of age) animals.

An ensuing morphological study in the cochlea of prenatal embryos showed a progressive reduction of the scala media from embryonic day (E) 35 and its complete absence by E50. The degeneration of hair cells was first observed at E50 and onwards. The immature stria vascularis failed to transform into a multilayered epithelium but consisted of one layer of underdeveloped/degenerated marginal cells. Strial intermediate cells were sparsely distributed in the spiral ligament and showed signs of degeneration. Strial basal cells were not easily recognized. RT-PCR analysis of the expression of genes regulating strial melanocyte development showed that *Pax3* mRNA was remarkably decreased in the cochlear lateral wall but remained intact in the diaphragm muscle and skin tissue.

The loss of the endolymphatic compartment in the *gw/gw* cochlea suggests a disruption of cochlear fluid and ion homeostasis. The mRNA and protein expression of several key players in cochlear homeostasis were thus investigated in the cochlear lateral wall by semi-quantitative RT-PCR and immunohistochemistry. RT-PCR analysis showed a significant reduction in expression of the strial intermediate cell-specific gene *Dct* and the tight junction gene *Cldn11* in the *gw/gw* cochlear lateral wall. Immunohistochemical analysis of the *gw/gw* cochlea showed loss of the tight junction protein CLDN11 in strial basal cells from E40, loss of the potassium channel subunit KCNJ10 in strial intermediate cells from E50, and loss of the Na-K-Cl cotransporter SLC12A2 in strial marginal cells from E50.

In conclusion, dysfunctional strial cells, in particular intermediate cells, fail to maintain the integrity of the stria vascularis and eradicate the main cochlear K^+ recycling pathway in the German waltzing guinea pig inner ear, ultimately resulting in the disruption of cochlear homeostasis and cochlear degeneration.

Key words: Cochlea; Deafness; Embryonic development; Inner ear; Kir4.1; Melanocyte; *Pax3*, Phenotype; Recessive genes; Recycling; Stria vascularis

LIST OF PUBLICATIONS

This thesis is based on the following papers, which are referred to in the text by their Roman numerals:

I. **Jin Z**, Mannström P, Skjönsberg Å, Järlebark L, Ulfendahl M. (2006) Auditory function and cochlear morphology in the German waltzing guinea pig. *Hear Res, 219: 74-84.*

II. **Jin Z**, Mannström P, Järlebark L, Ulfendahl M. (2006) Dysplasia of the stria vascularis in the developing inner ear of the German waltzing guinea pig. *Submitted to Cell Tissue Res.*

III. **Jin Z**, Wei D, Järlebark L. (2006) Developmental expression and localization of KCNJ10 K^+ channels in the guinea pig inner ear. *NeuroReport, 17: 475-479.*

IV. **Jin Z**, Ulfendahl M, Järlebark L. (2006) Disruption of cochlear homeostasis in the developing inner ear of the German waltzing guinea pig: Molecular and cellular studies. *Submitted to J Neurosci Res.*

PREFACE

This thesis describes the most recent findings on a long and winding path to unravel the full story behind the inborn deafness of the German waltzing guinea pig. I believe that this thesis will most definitely be read through by the dissertation opponent and thesis committee, and hopefully some of my colleagues (you had better read it!), but it is not very likely to reach a more general audience. However, for you, and those laymen who may not be familiar with auditory neuroscience and still find their way to these pages, the introduction section will provide some essential information as well as some clues to why these studies were performed and the papers written, and why studies like these should be done in the future. I sincerely hope that all readers will find this a fascinating, albeit seemingly never-ending story... just like I do.

Zhe Jin, Stockholm

CONTENTS

LIST OF ABBREVIATIONS

+/+	Wild-type animal(s)
ABR	Auditory brainstem response
ANOVA	Analysis of variance between groups
Ca^{2+}	Calcium ion
Cl^-	Chloride ion
CSF	Cerebrospinal fluid
Dct	Dopachrome tautomerase
E	Embryonic day
EP	Endocochlear potential
gw/+	Heterozygous animal(s) of the German waltzing guinea pig strain
gw/gw	Homozygous animal(s) of the German waltzing guinea pig strain
HCO_3^-	Bicarbonate ion
K^+	Potassium ion
KID	Keratitis-ichthyosis-deafness
oc	Organ of Corti
P	Postnatal day
rm	Reissner's membrane
RT-PCR	Reverse transcriptase-polymerase chain reaction
SGN	Spiral ganglion neuron(s)
SM	Scala media
SSH	Suppression subtractive hybridization
ST	Scala tympani
Stv	Stria vascularis
SV	Scala vestibuli
TUNEL	Terminal transferase dUTP nick end labeling

1 INTRODUCTION

The mammalian ear is a unique sensory system to perceive sound in the environment. It is composed of three major portions: the outer, middle and inner ear (Fig. 1). Each portion exerts a specific function in the hearing processes. The outer ear includes the auricle and the external auditory canal, which collects and transfers sound to the middle ear. The middle ear is an air-filled cavity containing the tympanic membrane and three tiny bones known as the ossicles (malleus, incus, and stapes), which serve as a mechanical lever that amplifies the vibration of tympanic membrane into the pressure wave in the inner ear. Deeply embedded inside the temporal bone, the inner ear constitutes the hearing (cochlea) and balance (vestibule and three semicircular canals) organs. These sensory organs of the inner ear are filled with fluids and contain sensory receptor cells – hair cells.

How can we hear? Sound waves are captured by the auricle and travel through the external auditory canal to vibrate the tympanic membrane. The vibrations are conducted to the oval window of the cochlea via the ossicle chain. The subsequent movement of the oval window creates pressure waves in the cochlear fluids and causes the basilar membrane to vibrate. Sensory hair cells sense the mechanical vibration and convert it into electrical signals. These signals are delivered by the auditory nerve up to the brain, where the signals are interpreted as sound.

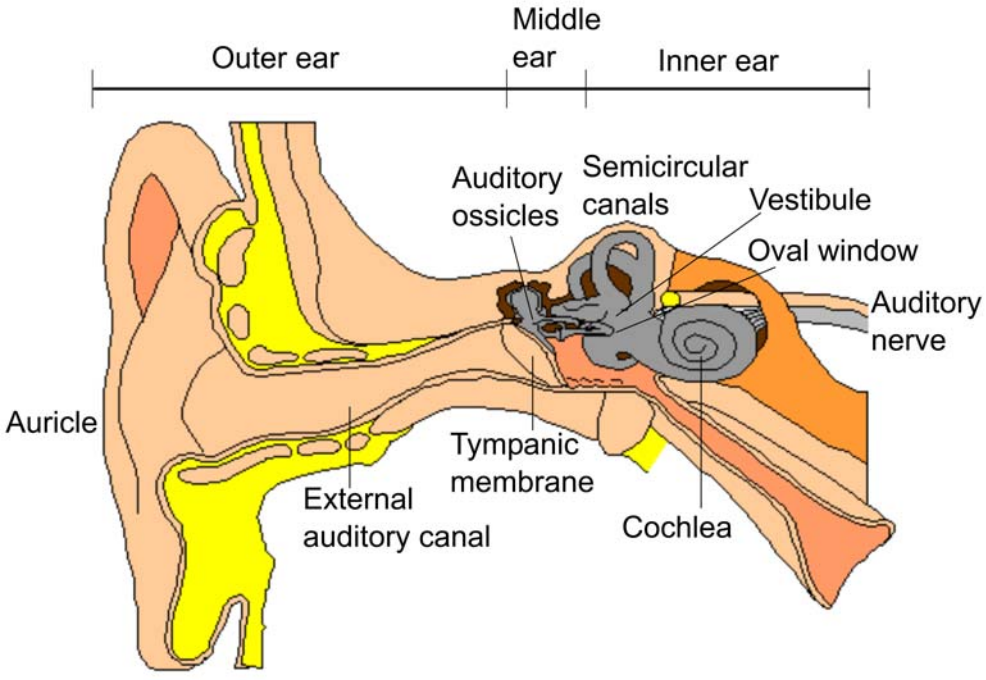

Figure 1. Anatomy of the human ear consisting of the outer, middle and inner ear. The inner ear contains the sensory organs for hearing (cochlea) and balance (vestibule and semicircular canals). (adapted from http://www.gpc.edu/~jaliff/anasense.htm)

1.1 MAMMALIAN COCHLEA – HEARING ORGAN

1.1.1 General cochlear anatomy

The mammalian cochlea is a snail-shaped, fluid-filled structure divided by two thin membranes into three parallel compartments: scala tympani, scala vestibuli and scala media (cochlear duct) (Fig. 2). Scala media, containing high [K^+] endolymph, is separated from scala vestibuli by the Reissner's membrane and from scala tympani by the basilar membrane. Scala tympani and scala vestibuli, filled with perilymph, are connected by a small opening at the cochlear apex, also known as helicotrema. The mechanoreceptive sensory epithelium, the organ of Corti, resides within scala media on the basilar membrane and extends throughout the length of the cochlea. It contains two types of sensory hair cells: one single row of inner hair cells and three rows of outer hair cells which are separated and surrounded by various supporting cells. On the apical surface of hair cells, actin-based cellular protrusions, stereocilia, are arranged in graded heights to serve as mechanoelectrical transducers. The tectorial membrane, which is a gelatinous structure, is attached primarily to the tips of stereocilia. Extending from primary auditory neurons (spiral ganglion neurons), the nerve fibers mainly contact on the basal surface of hair cells. Spiral ganglion constitutes two types of neurons (type I and type II), which bring electrical signals from hair cells to the brain. Located on the cochlear lateral wall are two non-sensorineural components, the stria vascularis and spiral ligament. The stria vascularis is a multilayered secretory epithelium, while the adjacent spiral ligament is a connective tissue structure containing five subtypes of fibrocytes. Both sensorineural and non-sensorineural components within the cochlea are indispensable for the normal hearing function.

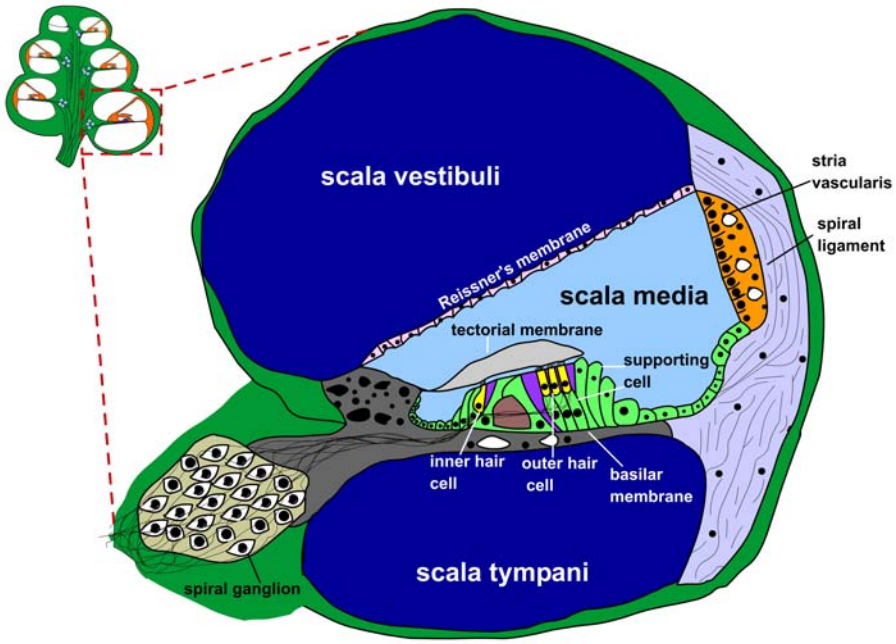

Figure 2. The schematic diagram illustrating a cross-section view of the cochlea. The cochlea is divided into three fluid-filled compartments: the scala vestibuli, media and tympani. The organ of Corti containing sensory hair cells resides within the scala media on the basilar membrane. The spiral ganglion has two types of primary auditory neurons (type I and II). The stria vascularis and the adjacent spiral ligament are situated along the cochlear lateral wall. (adapted from Jin and Duan 2006)

1.1.2 Cellular structure of stria vascularis and its development

The stria vascularis is a highly vascularized epithelium with high secretory and metabolic activity, which is mainly composed of marginal, intermediate and basal cells together with capillary endothelial cells (Fig. 3). The characteristic cellular architecture of the mature stria vascularis appears quite similar across different mammalian species, including mouse (Smith 1957), cat (Hinojosa and Rodriguez-Echandia 1966), guinea pig (Engström et al. 1955), and human (Kimura and Schuknecht 1970a; Kimura and Schuknecht 1970b). The luminal side of stria vascularis facing the scala media is composed of ectoderm-derived marginal cells, which possess extensive basolateral membrane infoldings and a rich population of mitochondria. On the other side of stria vascularis, the mesoderm-derived basal cells are spindle shaped, arranged tangentially and form a continuous barrier layer separating the stria vascularis from the adjacent spiral ligament. The intermediate cells are neural crest-derived melanocytes, which can easily be identified by their melanin pigments. The intermediate cells as well as blood capillaries are sandwiched between the marginal and basal cell layers. Between the adjacent marginal cells and basal cells are tight junctions, which insulate the stria vascularis as a unique compartment.

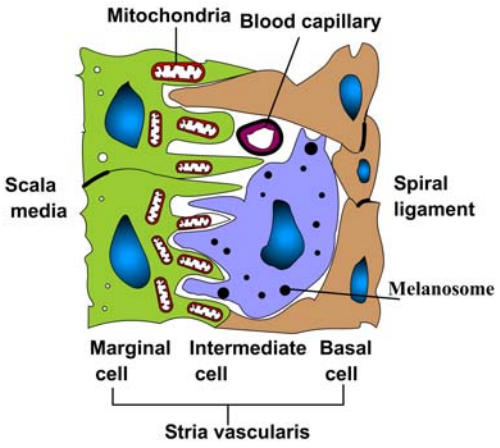

Figure 3. The cellular architecture of the mature stria vascularis (paper II).

The morphogenesis of the stria vascularis has been extensively described in humans (Chiba and Marcus 2000; Lavigne-Rebillard and Bagger-Sjöbäck 1992) and other mammals including guinea pigs both *in vivo* (Fernandez and Hinojosa 1974; Kikuchi and Hilding 1966; Thorn and Schinko 1985) and *in vitro* (Mou et al. 1997; Ågrup et al. 1996). The development of the stria vascularis in different species usually occurs with the successive appearance of the marginal, intermediate and basal cells and follows a base-to-apex gradient along the cochlear spiral, although the total time period of development varies among species. The primordial stria vascularis can be distinguished as a multilayered epithelium composed of undifferentiated cells. A condensation of mesenchymal cells develops adjacent to the epithelial layer and a continuous basal lamina lies in between. The first signs of early differentiation in the stria vascularis are the onset of basal lamina degradation and the presence of identifiable intermediate cells (melanocytes). Marginal cells within the epithelial layer appear more cuboidal in shape, and future basal cells are orientated in parallel to the surface of the developing stria vasularis. When the basal lamina is largely degraded and more intermediate cells are incorporated, the marginal cells develop their cellular projections containing a certain number of mitochondria toward the intermediate and basal cells. The flattened basal cells form a distinct layer separating the stria vascularis from the adjacent spiral ligament. Blood capillaries are also packed in the stria vascularis. As the interdigitation between different strial cells proceeds, the stria vascularis finally develops to its mature

form. The migration of melanocytes from the neural crest to the stria vascularis is essential for the development and interaction of other strial cells (Cable et al. 1992; Steel and Barkway 1989).

1.2 FLUIDIC AND IONIC HOMEOSTASIS IN THE COCHLEA

1.2.1 Cochlear fluids and endocochlear potential

The cochlea is a unique organ with respect to the different extracellular fluids filling it. Cochlear fluids play major roles in cochlear physiology such as transmission of the mechanical stimulus to the hair cells. Three major extracellular fluids have been identified in the cochlea: endolymph, perilymph and intrastrial fluid (Wangemann and Schacht 1996). The chemical composition varies greatly between the cochlear fluids (table 1).

Table 1. Chemical composition and electrical potential of the cochlear fluids (adapted from Wangemann and Schacht 1996).

	Endolymph of SM	Perilymph of SV	Perilymph of ST	Intrastrial fluid	CSF	Plasma
K^+ (mM)	157	6	4.2	2	3.1	5
Na^+ (mM)	1.3	141	148	85	149	145
Ca^{2+} (mM)	0.023	0.6	1.3	0.8	-	2.6
Cl^- (mM)	132	121	119	55	129	106
HCO_3^- (mM)	31	18	21	-	19	18
Protein (g/l)	0.38	2.42	1.78	-	0.24	42.38
pH	7.4	7.3	7.3	-	7.3	7.3
Potential (mV)	~80-100	<3	0	~100	0	0

SM, scala media; SV, scala vestibuli; ST, scala tympani; CSF, cerebrospinal fluid.

The perilymph is a typical extracellular fluid, and its ionic composition is similar but not identical to that of plasma and cerebrospinal fluid. The dominant cation in the perilymph is sodium. Both scala vestibuli and scala tympani are filled with perilymph which communicates at the cochlear apex via the helicotrema. However, the perilymph of scala vestibuli and scala tympani differs in composition and origin (Sterkers et al. 1988): the perilymph of scala vestibuli originates mainly from plasma across a blood-perilymph barrier, whereas the perilymph of scala tympani is partially formed by cerebrospinal fluid (CSF). The movement of perilymph in response to vibration of oval window membrane causes the motion of basilar membrane and in turn hair cell stimulation.

The endolymph is a unique extracellular fluid with unusually high [K^+] but low [Na^+] and [Ca^{2+}]. Enclosed in scala media, the endolymph has direct contact with several different epithelial cell types including sensory hair cells. It is well known that the endolymph originates from the perilymph through the labyrinthine epithelium, rather than from blood plasma (Konishi et al. 1978; Sterkers et al. 1982). Interestingly, the endolymph in scala media possesses a large positive transepithelial potential with respect to perilymph and plasma, designated as the endocochlear potential (EP). The EP was first recorded by von Békésy (Békésy 1951) and its magnitude is around 80-

100mV in the mammalian cochleas studied. However, no such high potential has been detected in the vestibular endolymphatic labyrinth or any other mammalian organ. The EP in the cochlea is generally considered to be generated by stria vascularis (Békésy 1951; Tasaki and Spyropoulos 1959) and to serve as a major driving force for sensory transduction. The spiral ligament might also contribute to the generation or maintenance of EP as evidenced by a dramatic reduction of EP in *Pou3f4*-deficient mice with defect of spiral ligament fibrocytes (Minowa et al. 1999). Several electrophysiological models have been proposed to explain the mechanism underlying the EP generation (Marcus and Thalmann 1980; Offner et al. 1987; Salt et al. 1987). Nevertheless, the molecular substrate that produces EP has only been identified until very recently. The EP is essentially generated by the potassium channel subunit KCNJ10 (Kir4.1) located in the intermediate cells of stria vascularis (Marcus et al. 2002; Takeuchi et al. 2000).

The intrastrial fluid fills the narrow intrastrial compartment, which is isolated from perilymph in the spiral ligament and endolymph in the scala media by basal and marginal cell layers, respectively. The ionic composition of the intrastrial fluid resembles that of the perilymph containing low [K^+] but relatively high [Na^+]. Notably, the intrastrial fluid also maintains a positive voltage potential of ~100 mV relative to the perilymph. It is referred to as intrastrial potential (Salt et al. 1987) and has been assumed as a source of EP.

1.2.2 Cochlear potassium recycling and its molecular correlates

In the cochlea, K^+ ions provide major charge carriers for hair cell transduction as well as for the EP production. Therefore, cochlear K^+ homeostasis is essential for maintaining high sensitivity of hair cells and thus for normal hearing function. It has been shown by radioactive tracer experiment that K^+ ions in the endolymph are derived from perilymph rather than from blood plasma (Konishi et al. 1978). The different epithelial cells lining scala media are coupled by tight junctions, which limit extracellular diffusion of K^+ ions between endolymph and perilymph. An ensuing question arises as to how K^+ ions are recycled from perilymph back to endolymph. Several putative routes for K^+ recirculation in the cochlea have been proposed so far (Fig. 4) (Kikuchi et al. 2000a; Wangemann 2002a; Wangemann 2002b; Weber et al. 2001). Driven by the high endocochlear potential, K^+ ions in the endolymph pass through the apical mechanotransduction channels into the sensory hair cells, and then exit the hair cells via K^+ channels (e.g. Kcnq4, Kcnn2 and Kcnma1) along the their basolateral membranes (Kros 1996). The released K^+ ions are subsequently taken up by surrounding supporting cells via potassium channels and transporters (e.g. K-Cl cotransporters Kcc3 and Kcc4). With aid of gap junction systems, the K^+ ions are further transported either medially toward the spiral limbus and back to endolymph (Spicer and Schulte 1998), or laterally toward the spiral ligament (Kikuchi et al. 1995). Alternatively, K^+ ions can flow through the perilymph above or below the scala media, or through outer sulcus cells toward the spiral ligament (Chiba and Marcus 2000; Zidanic and Brownell 1990). The epithelial cell system and the connective tissue cell system are two independent gap junction networks in the cochlea, which are mainly composed of GJB2, GJB3 and GJB6. It has been thought that both gap junction

networks are participating in cochlear K^+ recirculation pathway by providing intercellular transport routes (Kikuchi et al. 2000b). Through gap junction networks, K^+ ions are delivered to the stria vascularis and released from the intermediate cells via the KCNJ10 channel into the intrastrial compartment. From there K^+ ions were taken up by the basolateral Na-K-Cl cotransporter (Slc12a2) and Na-K-ATPase (Atp1a1/Atp1b2) and secreted back into endolymph by the apical Kcnq1/Kcne1 potassium channel of the marginal cells.

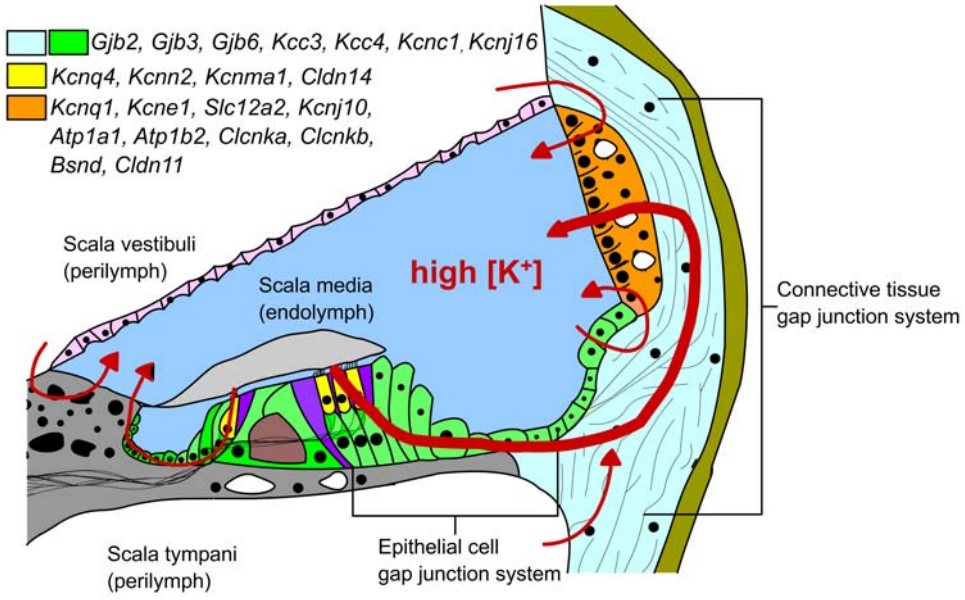

Figure 4. Schematic illustration of cochlear K^+ recycling pathway and the distribution of key molecular players in the cochlea. *Gjb2*, gap junction protein, beta 2; *Gjb3*, gap junction protein, beta 3; *Gjb6*, gap junction protein, beta 6; *Kcc3 (Slc12a6)*, solute carrier family 12, member 6; *Kcc4 (Slc12a7)*, solute carrier family 12, member 7; *Kcnc1*, potassium voltage gated channel, Shaw-related subfamily, member 1; *Kcnj16*, potassium inwardly-rectifying channel, subfamily J, member 16; *Kcnq4*, potassium voltage-gated channel, subfamily Q, member 4; *Kcnn2*, potassium intermediate/small conductance calcium-activated channel, subfamily N, member 2; *Kcnma1*, potassium large conductance calcium-activated channel, subfamily M, alpha member 1; *Cldn14*, claudin 14; *Kcnq1*, potassium voltage-gated channel, subfamily Q, member 1; *Kcne1*, potassium voltage-gated channel, Isk-related subfamily, member 1; *Slc12a2*, solute carrier family 12, member 2; *Kcnj10*, potassium inwardly-rectifying channel, subfamily J, member 10; *Atp1a1*, ATPase, Na+/K+ transporting, alpha 1 polypeptide; *Atp1b2*, ATPase, Na+/K+ transporting, beta 2 polypeptide; *Clcnka*, chloride channel Ka; *Cldnkb*, chloride channel Kb; *Bsnd*, Bartter syndrome, infantile, with sensorineural deafness (Barttin); *Cldn11*, claudin 11.

An array of functional proteins including ion channels, cotransporters, ATPases, and intercellular junctions are actively participating the cochlear K^+ recycling pathway (Fig. 4 and 5). The dysfunction of these key regulators is associated with deafness in humans and mouse mutants.

Kcnq1 and *Kcne1* encode the α- and β-subunits of K^+ channel, respectively. These protein subunits co-assemble to form functional channels and have been detected in the apical membrane of strial marginal cells and vestibular dark cells (Neyroud et al. 1997;

Nicolas et al. 2001; Sakagami et al. 1991). Additionally, Kcnq1/Kcne1 K^+ currents were also recorded in both cell types. Kcnq1/Kcne1 K^+ channel is by far the sole functional element to secret K^+ ion across the apical membrane of marginal cells. The essential role of Kcnq1/Kcne1 K^+ channel for K^+ secretion in the cochlea was clearly illustrated in the mouse mutants with a targeted deletion of either *Kcnq1* or *Kcne1* gene (Lee et al. 2000; Vetter et al. 1996). Genetic mutations affecting either *KCNQ1* or *KCNE1* are responsible for cardioauditory syndrome (Jervell and Lange-Nielsen syndrome) (Neyroud et al. 1997; Schulze-Bahr et al. 1997).

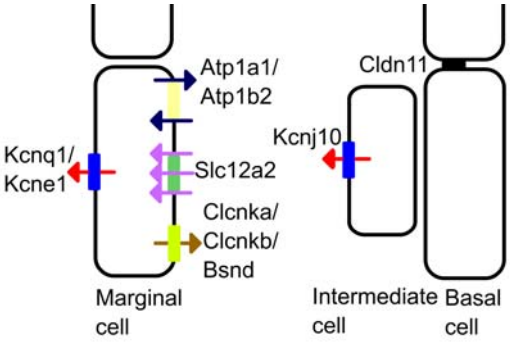

Figure 5. The cellular localization of key ion transport apparatuses in the stria vascularis.

Slc12a2 encodes a Na-K-Cl cotransporter which is primarily expressed in the basolateral membrane of strial marginal cells and vestibular dark cells (Crouch et al. 1997). In the cochlea, Slc12a2 is important for effective uptake of K^+ from the intrastrial compartment. K^+ secretion from the stria vascularis was abolished in mice with *Slc12a2* mutations (Delpire et al. 1999; Dixon et al. 1999). However, no human deafness related to mutations in *SLC12A2* gene has been yet identified.

Kcnj10 (Kir4.1), an inward rectifier K^+ channel subunit is specifically expressed in the strial intermediate cells (Ando and Takeuchi 1999). The time course of its developmental expression was closely correlated to the elevation of EP (Hibino et al. 1997). Loss of EP and partial reduction of cochlear endolymphatic volume and $[K^+]$ in the *Kcnj10*-null mice (Marcus et al. 2002), indicate that Kcnj10 channel is essential for EP generation and play a major role in the cochlear K^+ recycling pathway.

Claudin 11 encoded by *Cldn11* gene, a member of the claudin family, is an integral membrane protein and one component of tight junction strands. It is exclusively localized between strial basal cells in the cochlea (Kitajiri et al. 2004b). Claudin 11 co-assembling with other tight junction components connects strial basal cells and forms a continuous barrier separating intrastrial fluid from the perilymph in the spiral ligament. The important role of Claudin 11 in the maintenance of the electrically isolated intrastrial compartment is evidenced by depression of EP in the *Cldn11*-null mice (Gow et al. 2004; Kitajiri et al. 2004a).

Connexin 26 (Gjb2), one of major gap junction proteins, is abundantly distributed in both the epithelial cell and connective tissue gap junction systems in the cochlea. Gap junctions, especially connexin 26, provide an intercellular passage for cochlear K^+ ions and therefore are essential for cochlear function. Mutations in the *GJB2* gene account for about 50% autosomal recessive non-syndromic deafness (DNFB1) (Zelante et al. 1997). Two independent transgenic mouse mutants with the mutated *Gjb2* gene (Cohen-Salmon et al. 2002; Kudo et al. 2003) display hearing loss, but the EP as well

as the endolymphatic [K^+] and volume is not altered. It suggests that Gjb2 might not be essential for EP production and cochlear K^+ recirculation.

1.2.3 Strial melanocyte and its functional role

Melanocytes have been identified in various sites of the inner ear including the stria vascularis, the cochlear modiolus as well as specific locations of the vestibular end organs (Meyer zum Gottesberge 1988). Generally, otic melanocytes originate from the embryonic neural crest (Hilding and Ginzberg 1977). Their precursors, melanoblasts, migrate from neural crest to the inner ear during early development and ultimately differentiate into melanocytes. The melanoblast is an unpigmented cell, but it can be identified with a marker dopachrome tautomerase (Dct) (Steel et al. 1992). In the stria vascularis, the melanocytes, also known as intermediate cells, contain melanin pigments and extend dendritic processes to interdigitate with adjacent marginal and basal cells. It has been showed that there are two forms of intermediate cells present in the mouse stria vascularis: light and dark intermediate cells (Cable and Steel 1991). The light intermediate cells which are present from birth contain large amount of organelles but very few melanin pigments, whereas the dark intermediate cells which are only observed in the adult stria vascularis, are more heavily pigmented and exhibit pynotic nuclei and contain few organelles. These dark intermediate cells are presumed to be a degenerate form of the light ones.

What is the exact role of strial melanocytes in cochlear function? Although it is still not fully understood, the putative roles of strial melanocytes include 1) normal structural development of stria vascularis. The migration of melanocytes into the stria vascularis is important for the differentiation of marginal cells, the interdigitation between the marginal and basal cells as well as the sustainment of strial capillary network, as evidenced by the findings in the stria vascularis of melanocyte-deficient mutant animals (Hoshino et al. 2000; Steel and Barkway 1989). 2) generation and maintenance of EP. In the dominant white spotting (*W*) mutant mice which did not contain strial melanocytes, no EP was generated (Steel et al. 1987). In addition, the presence of strial melanocytes is constantly correlated with a measurable EP (Cable et al. 1994). In mutant mice displaying a progressive degeneration of strial melanocytes (e.g. B^{lt} light mutant mice), the EP gradually decreased with age (Cable et al. 1993). It indicates that the continued presence of strial melanocytes is required for the maintenance of EP. Interestingly, the EP is independent of the pigment production ability of strial melanocytes since albino animals still have a normal EP despite of the presence of amelanotic melanocytes in the stria vascularis.

A complex molecular network composed of various genes is participating in the different aspects of strial melanocytes development (proliferation, migration, survival and differentiation) (Fig. 6) (Price and Fisher 2001; Tachibana 2001). The reciprocal interaction between these regulatory genes has been extensively studied. Proto-oncogene *Kit* and its ligand *Kitl* are necessary for the survival and/or migration of melanoblasts (Wehrle-Haller 2003). Dominant white spotting (*W*) and Steel (*Sl*) mutant mice, which have the mutation in the *Kit* and *Kitl* genes respectively, lack strial melanocytes and thus cause hearing impairment (Cable et al. 1994; Cable et al. 1995;

Schrott et al. 1990; Steel et al. 1992). Endothelin 3 (*Edn3*) and its receptor *Ednrb*, transcription factors *Pax3*, *Sox10*, and *Mitf* have also been considered indispensable for the migration, differentiation, and proliferation of melanoblasts and melanocytes. Among these genes, *Mitf* plays a central role in the development and function of melanocytes (Price and Fisher 2001; Tachibana 2001). Mutations in the human *EDN3*, *EDNRB*, *PAX3*, *SOX10* and *MITF* genes result in the hearing loss of several subtypes of Waardenburg (auditory-pigmentary) syndrome (Pingault et al. 1998; Read and Newton 1997).

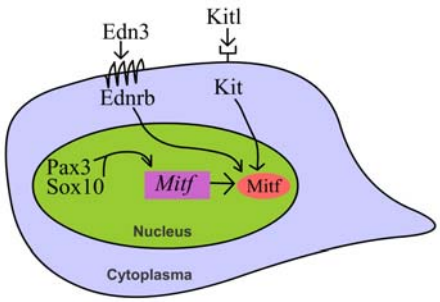

Figure 6. Part of the molecular network regulateing melanocyte development. *Mitf* gene (purple) and its protein (red) are master regulators.

1.3 ANIMAL MODELS FOR HUMAN HEREDITARY HEARING IMPAIRMENT

Human genetic hearing loss is a highly diverse sensory disorder. It accounts for more than 50% of deafness cases. The loss of hearing could be present as the only clinical manifestation (non-syndromic deafness) or as part of a syndrome (syndromic deafness). To date, at least 400 different types of genetic deafness have been described. Over the last decade, there has been an astonishing progress in exploring the molecular correlate for each type of genetic deafness. More than 100 different genes and many more loci have been identified to be involved in genetic hearing loss. An up-to-date and comprehensive summary of hereditary hearing loss and the causative gene can be viewed at the Hereditary Hearing Loss Homepage (http://webhost.ua.ac.be/hhh/).

However, the limited access to the human inner ear and availability of human temporal bone specimens, impedes further understanding of human pathology of inherited deafness and the underlying molecular mechanisms. In addition, developmental studies and detailed electrophysiological analysis such as endocochlear potential measurements are not readily carried out in human inner ears. In contrast, animal models do not have these disadvantages and especially those animal mutants closely mimicking human hearing disorders are proving extremely useful to aid in the discovery of human deafness genes. A typical example is that the discovery of mouse gene *Myo15a* for shaker 2 (*sh2*) mutants leads to the identification of the orthologous human gene MYO15A and human deafness loci for DFNB3 (Wang et al. 1998). Among the different animal models, the mouse has long been considered as a major choice of model in the field of auditory research. It has several advantages such as a short gestation period of around 3 weeks and the applicability of genetic manipulation technologies. According to studies on inner ear pathology of deaf mouse mutants, they can be mainly classified into several groups (Steel 1995): 1) morphogenetic defects, e.g. fibroblast growth factor 3 (*Fgfr3*) knockout mice. 2) peripheral neural defects, e.g. Neurotrophin receptor B (*Trkb*) knockout mice. 3) neuroepithelial defects, e.g. Shaker 1 (*sh1*) mice. 4) cochleosaccular defects (abnormal endolymph homeostasis), e.g. potassium channel gene *Kcnq1* knockout mice. 5) membrane matrix defects, e.g. alpha

tectorin gene (*Tecta*) knockout mice. This thesis primarily focused on animal mutants with cochleosaccular defects.

1.3.1 Animal mutants with abnormal endolymph homeostasis

A specific type of human inner ear defect also known as Scheibe's dysplasia (cochleosaccular defect) was first described in congenitally deaf patients (Scheibe 1892). This is caused by the underdevelopment of the inferior part of the membranous labyrinth which forms the cochlear duct and saccule, although the bony labyrinth is fully developed (Ormerod 1960). Despite the presence of some variability, the typical cochlear pathology in Scheibe's dysplasia/cochleosaccular defect includes a primary stria vascularis defect, reduction/absence of cochlear duct, and variable loss of sensory hair cells and spiral ganglion neurons, indicative of abnormal endolymph homeostasis (Fig. 7). Scheibe's dysplasia is the most common form of inner ear aplasia associated with congenital deafness in humans (Paparella and Schachem 1991). It is more frequently observed in temporal bones of patients with syndromic deafness, such as Waardenburg (auditory-pigmentory), Usher (auditory-visual), and Jervell and Lange-Nielsen (cardioauditory) syndromes. The molecular correlates for several types of syndromic deafness have been disclosed recently (Willems 2004). However, cochleosaccular defect is rarely associated with non-syndromic hearing loss.

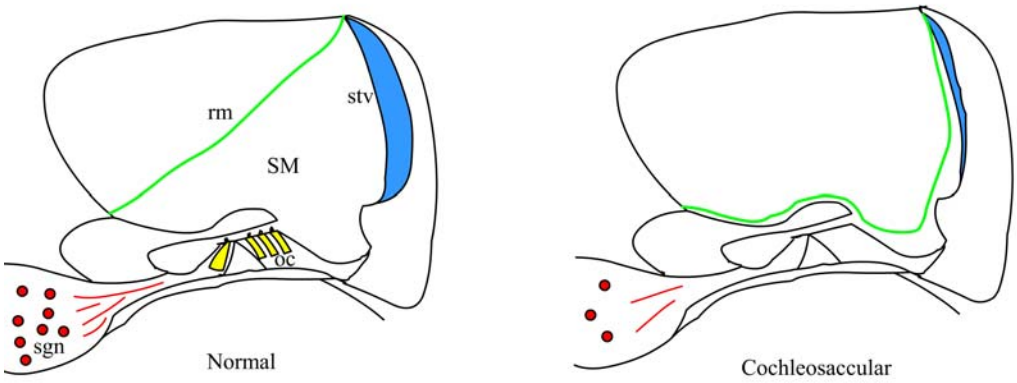

Figure 7. Typical cochlear pathology of Scheibe's dysplasia / cochleosaccular defect: primary defect in the stria vascularis (stv), sometimes collapse of Reissner's membrane (rm), secondary degeneration of sensory hair cells and spiral ganglion neurons (sgn). SM, scala media; oc, organ of Corti. (adapted from Steel 1995)

Cochleosaccular defects have been widely reported in a variety of animal species including cat, dog, rat and mouse (table 2). Although there are both intra- and interspecies differences in cochlear pathology, descent of Reissner's membrane, cochlear duct reduction and atrophy of the stria vascularis are still early and prominent features.

One group deaf animal mutants (only mice so far as I know) carries mutated or eliminated version of target genes which are known to be essential for cochlear K^+ recirculation, such as *Kcnq1*, *Kcne1*, *Slc12a2* and *Kcnj10*. In these postnatal mouse mutants, the endocochlear potential (EP) was reduced or abolished; the cochlear duct

was diminished to a variable degree following the collapse of Reissner's membrane. However, it is not necessary that all the mouse mutants with targeted disruption of genes involved in cochlear ionic homeostasis display the same cochleosaccular pathology. As an example, no obvious morphological malformation was detected in the cochlea of tight junction gene *Cldn11*-null mouse despite of the reduced EP (Gow et al. 2004; Kitajiri et al. 2004a).

The other group of deaf animal mutants is associated with melanocyte defects in the stria vascularis as well as in the skin. Therefore, they usually have abnormal coat color, such as white spots or patches. Deaf white cats, Dalmatian dogs, white spotting (*W*) rats and Steel (*Sl*) mice are well-known examples of animals with pigment-associated deafness (table 2). Interestingly, the absence of strial melanocytes, the lack of EP and the resulting hearing loss can be highly variable between and within each individual animal: some cochleas have no strial melanocyte and no detectable EP, while in other cochleas strial melanocytes are present only in the pigmented portion of the stria vascularis and a reduced EP can be measured (Cable et al. 1994).

Table 2. Animal mutants with cochleosaccular defects

Mutant name	Gene	Origin	Inheritance	References
Kcnq1$^{-/-}$ mice	*Kcnq1*	T	R	1, 2
Kcne1$^{-/-}$ mice Punk rocker	*Kcne1*	T, S	R	3, 4
Slc12a2$^{-/-}$ mice Shaker-with-syndactylism mice	*Slc12a2*	T, S	R	5, 6, 7
Kcnj10$^{-/-}$ mice	*Kcnj10*	T	R	8, 9
VGA-9 mice Microphthalmia mice *JF1* mice	*Mitf*	T, S	R, SD	10, 11,12
WS4 mice Piebald mice	*Ednrb*	S, T	R	13, 14, 15
Steel mice	*Kitl*	S	SD	16, 17
Dominant spotting mice	*Kit*	S	SD	18, 19
Lethal spotting mice *Edn3*$^{-/-}$ mice	*Edn3*	S, T	R	20, 21
Splotch mice	*Pax3*	S	SD	22, 23
White spotting rats	*Kit*	S	R	24, 25, 26
Deaf white cats	Unknown	S	D	27, 28
Dalmatian dogs	Unknown	S	Unknown	29, 30

Origin: T, transgenic and knockout; S, spontaneous. Inheritance: R, recessive; D, dominant; SD, semidominant. References: 1, (Lee et al. 2000); 2, (Rivas and Francis 2005); 3, (Vetter et al. 1996); 4, (Letts et al. 2000); 5, (Delpire et al. 1999); 6, (Dixon et al. 1999); 7, (Pace et al. 2001); 8, (Marcus et al. 2002) ; 9, (Rozengurt et al. 2003) ; 10, (Tachibana et al. 1992) ; 11, (Hodgkinson et al. 1993); 12, (Motohashi et al. 1994); 13, (Koide et al. 1998); 14, (Matsushima et al. 2002); 15, (Pavan and Tilghman 1994); 16, (Zsebo et al. 1990); 17, (Schrott et al. 1990); 18, (Deol 1970); 19, (Steel et al. 1987); 20, (Baynash et al. 1994); 21, (Mayer and Maltby 1964); 22, (Steel and Smith 1992); 23, (Buckiova and Syka

2004); 24, (Kitamura et al. 1994); 25, (Hoshino et al. 2000); 26, (Araki et al. 2002); 27, (Heid et al. 1998); 28, (Ryugo et al. 2003); 29, (Mair 1976); 30, (Branis and Burda 1985).

1.3.2 The German waltzing guinea pig

The guinea pig has been long established as an important animal model for research on cochlear physiology due to its frequency sensitivity and its larger cochlear size. Similar to humans, their cochlear structure and function have been fully developed *in uterus*. Newborn guinea pigs could hear at birth in contrast to those altricial mammals such as mice, cats and dogs, in which the final stage maturation of cochlea occurs postnatally. In addition, guinea pig as well as human populations are characterized by genomic heterogeneity, which is unendowed in most of deaf mice mutants occurring in large inbred populations. With the recent completion of low coverage guinea pig genome sequence (http://www.broad.mit.edu/mammals/) and advent of more advanced gene-manipulation techniques, it makes it possible in the near future to use guinea pigs as animal models to explore "deafness gene" for human hereditary hearing loss.

To my knowledge, there have been three known guinea pig strains displaying inherited hearing loss and typical waltzing behavior (table 3). The first strain of waltzing guinea pigs known as the Kansas strain was described already by Ibsen and Risty in 1929 as "Two related individuals with a tendency to whirl, or waltz, similar to that known in Japanese waltzing mice" (Ibsen 1929). The Kansas strain displayed an autosomal recessively inherited hearing loss already from birth. Cochlear morphology in the homozygous animals showed a normal position of Reissner's membrane but variable degeneration of sensory and neural structures (Lurie 1939; Lurie 1941). Another strain of waltzing guinea pigs, the NIH stain, has been extensively described by Ernston (Ernstson 1970; Ernstson 1971a; Ernstson 1971b; Ernstson 1972; Ernstson et al. 1969). The NIH strain followed an autosomal dominant inheritance with a recessive lethal effect (Ernstson 1970). The homozygotes displayed progressive hearing loss becoming more severe 14 days after birth (Canlon et al. 1993; Ernstson 1972). Loss of sensory hair cells was manifested at 2-3 months of age in the homozygotes, followed by degeneration of spiral ganglion neurons, although there was no detectable atrophy of stria vascularis. Stereocilia fusion and cuticular plate protrusion were major pathologies in both cochlear and vestibular hair cells. In addition, unique actin filament rods existed in type I vestibular hair cells of homozygous animals as revealed by transmission electron microscopy (TEM) observations (Sobin and Weraall 1983). Although the auditory function and inner ear pathology have been extensively studied, the causative genetic substrate has not yet been identified for either of the two strains of waltzing guinea pigs.

Table 3. Comparison of different strains of waltzing guinea pigs.

Strain Name	Inheritance mode	Mutated gene	Availability	Inner ear pathology	
				Cochlea	Vestibule
Kansas	AR	Unknown	No	Yes	No
NIH	AD, RL	Unknown	Yes	Yes	Yes
German	AR	Unknown	Yes	Yes	Yes?

AR, autosomal recessive, AD, autosomal dominant; RL, recessive lethal.

The third and most recently described strain of waltzing guinea pigs has also arisen spontaneously. It was originally discovered in an animal facility in Germany in 1996, thus named the German waltzing guinea pig. Two normal-behaving guinea pigs had a litter of four offspring, of which two animals (one male and one female) displayed a typical circling/waltzing behavior. These two waltzing guinea pigs were subsequently interbred and produced two litters of progenies, each comprised of two waltzing animals. All six waltzing guinea pigs were then transferred to Karolinska Institutet (Stockholm, Sweden). Systematical breeding of these waltzing animals together with normal guinea pigs from an outbred Swedish strain, revealed the autosomal recessive mode of inheritance (Skjönsberg et al. 2005; Ernstson, unpublished observation). However, the underlying genetic substrate is still unknown. Both homozygotes (*gw/gw*) and heterozygotes (*gw/+*) of the German waltzing guinea pigs are viable and fertile with normal body size and lifespan. They have pigmented eyes as well as normal coat color varying from yellowish to brown despite occasional white spots.

Heterozygotes (*gw/+*) of the German waltzing guinea pig can not be distinguished from wild-type guinea pigs in external appearance and cochlear morphology. Hearing threshold and endocochlear potential (EP) have been shown within a normal range in the heterozygous animals, which display normal behavior and vestibular reaction. Interestingly and paradoxically, they exhibit resistance to noise exposure, while more susceptible to ototoxic drugs (Halsey et al. 2005; Skjönsberg et al. 2005). The heterozygous German waltzing guinea pigs represent an intriguing animal group for investigating how exogenous (i.e. environmental) auditory stress factors reciprocally act with endogenous (i.e. genetic) elements.

Homozygotes (*gw/gw*) of the German waltzing guinea pig (Fig. 8) are readily recognized from their littermates at birth by their distinct circling behavior and head-tossing movement. The lack of Preyer reflex and auditory brainstem response (ABR) in neonatal *gw/gw* animals suggested they were deaf already (Skjönsberg et al. 2005). Preliminary histology study showed that scala media was diminished in the prenatal *gw/gw* animal. This finding indicates that cochlear fluid and/or ion homeostasis is severely disrupted in the inner ear of the *gw/gw* animal. In addition, the vestibular endolymphatic compartment was similarly collapsed. The work in this study focused on the cochlear portion of the homozygous German waltzing guinea pig (*gw/gw*). In papers I and II, the time course of cochlear degeneration in the postnatal and prenatal *gw/gw* animal was described in detail. The cellular and molecular basis for disruption of cochlear homeostasis in the developing *gw/gw* animal was presented in paper III and IV.

Figure 8. Young (postnatal day 21) homozygous German waltzing guinea pig (*gw/gw*) with yellow-brown coat color and pigmented eyes.

2 AIMS OF THE STUDY

The long-term goal of this project was to identify the molecular and genetic substrate for inner ear degeneration in the German waltzing guinea pig (*gw/gw*). The specific aims of the studies included in the thesis were:

- To characterize the cochlear pathology in the **postnatal** homozygous animals.
- To characterize the time course of cochlear degeneration and explore the underlying mechanism in the **prenatal** homozygous embryos/fetuses.
- To investigate the cellular and molecular basis of the disruption of cochlear homeostasis in the developing inner ear of the German waltzing guinea pig.

3 MATERIALS AND METHODS

3.1 EXPERIMENTAL ANIMALS AND TISSUE PREPARATIONS

3.1.1 Experimental animals

Guinea pigs used in the present study originated from two different strains (table 4). Homozygous (*gw/gw*) and heterozygous (*gw/+*) guinea pigs were derived from the German waltzing guinea pig strain, which are not commercially available and bred only at Karolinska Institutet. Heterozygous (*gw/+*) animals were identified by controlled breeding (Skjönsberg et al. 2005). Wild-type (+/+) guinea pigs used as control and for breeding purpose were derived from a commercially available guinea pig strain ("Sahlin strain"; Bio Jet Service, Uppsala, Sweden). Healthy and pigmented guinea pigs were selected for breeding to produce a sufficient number of embryos/fetuses.

Table 4. Different age of guinea pigs (embryos) used in the present study

Paper number	+/+	*gw/gw*	*gw/+*
I	Postnatal animals from newborn up to 2 years of age		
II	E25, E30, E40, E45, E50, E60, adult		Adult
III	E30, E35, E40, E45, E50, E60, P0, P60	−	−
IV	E30, E35, E40, E45, E50, E60, P0, adult		P0, adult

+/+, wild-type; *gw/gw*, homozygote; *gw/+*, heterozygote; E, embryonic day; P, postnatal day.

All animal experiments and procedures were approved by Swedish Animal Care and Use Committee (approvals N10/01, N11/01, N464/03, and N465/03). Animals were housed in an animal facility with free access to food and water under 12:12 h light dark cycle. As guinea pigs cannot manufacture their own vitamin C, ascorbic acid (vitamin C) was supplemented in the daily drinking water.

3.1.2 Tissue preparations

Postnatal guinea pigs were deeply anesthetized with an overdose sodium pentobarbital. For histological and immunohistochemical studies, the animals were transcardially perfused with 0.9% saline followed by ice-cold 4% formaldehyde fixative freshly prepared from paraformaldehyde. After decapitation, the temporal bones were removed and the cochleas were dissected out. Some cochleas were immersed in *RNAlater*™ RNA stabilization reagent (Qiagen) to avoid the potential RNA degradation, the cochlear bony capsule was stripped off and the cochlear lateral wall/stria vascularis was carefully detached from cochlear sensorineural structures (Fig. 9). Either the whole cochlea or the dissected cochlear lateral wall was further processed for total RNA isolation. The other cochleas were locally perfused with 4% paraformaldehyde fixative through the round window and a small hole at the apical turn, and then immersed in the same fixative (for light microscopy and immunohistochemistry) or 3% glutaraldehyde (for transmission electron microscopy) overnight at 4ºC. To prepare for cochlear cryosection and histological analysis, the cochleas were decalcified with 0.1 M EDTA made in 0.1 M phosphate buffer (PB) until the bony capsules were soft enough for the subsequent processing.

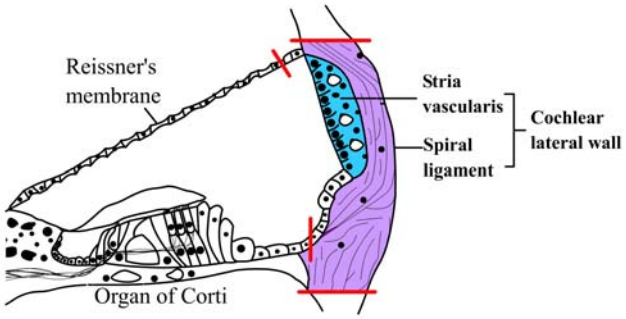

Figure 9. Schematic illustration of dissection of cochlear lateral wall tissue from the guinea pig inner ear.

Timed pregnant guinea pigs were sacrificed and the abdomen cavity was opened to expose the uterus. The embryos/fetuses were immediately taken out and sacrificed without transcardial perfusion. After dissected out from the temporal bones, the cochleas were processed following the same procedure as described above in the postnatal animals.

The tissue preparation procedure was illustrated in the following flow chart.

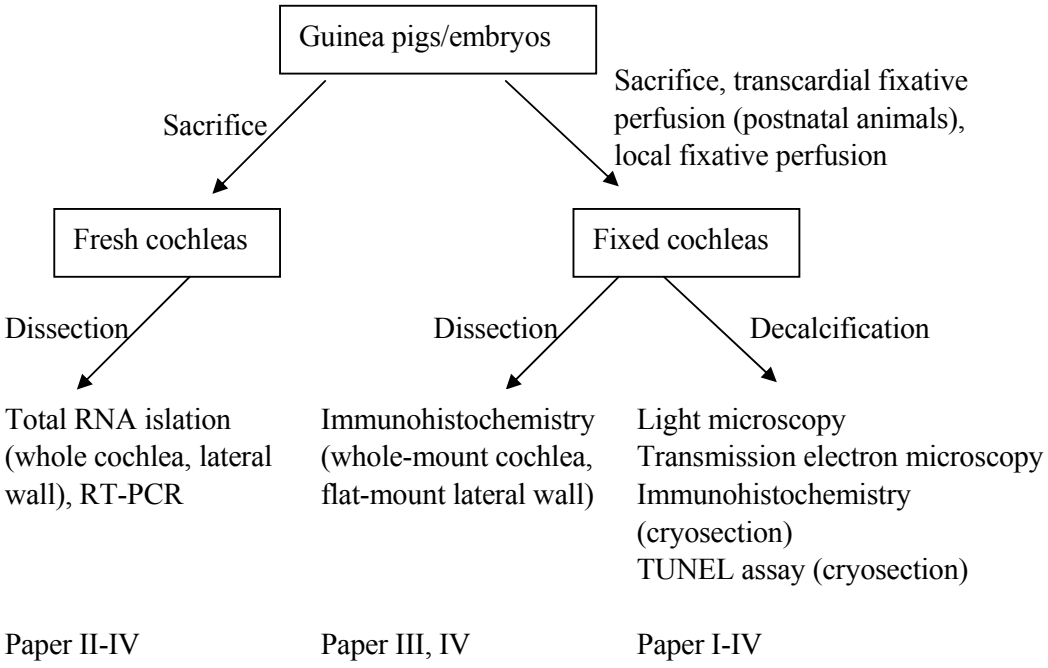

3.2 COCHLEAR HISTOLOGY ANALYSIS

3.2.1 Whole-mount and flat-mount morphology

The cochleas from neonatal guinea pigs were dehydrated with a graded methanol series (25%, 50%, 75%, and 100% methanol), and then cleared in a 1:2 mixture of benzyl alcohol: benzyl benzoate (Sigma). Cleared cochleas were examined and photographed under a dissecting microscope (Leica) equipped with a digital camera (JVC). The dissected cochlear lateral wall tissue strips were flat-mounted with the marginal cell side up in phosphate-buffered saline (PBS)/glycerol (1:1) on 8-well slides (Erie Scientific), and examined under a light microscope (Zeiss).

3.2.2 Light microscopy

The cochleas were washed in 0.1 M PB several times, dehydrated in a graded ethanol series and embedded in JB4 resin (Polyscience). The cochleas were sectioned at 4 or 5-μm thickness with a rotary microtome (Microm HM355S) along the midmodiolar plane. Every third section was mounted on glass slides, stained with 0.1% toluidine blue and examined under a light microscope (Zeiss).

3.2.3 Transmission electron microscopy

The cochleas were post-fixed in 1% osmium tetroxide, dehydrated in a graded series of ethanol, and embedded in plastic Agar 100 resin (Agar Scientific). After polymerization, the third cochlear turn was dissected out and re-embedded on a blank block of Agar 100 for sectioning. Sections at 1-μm thickness were cut on an ultratome (LKB Cryo Nova) and stained with toluidine blue in order to select angles and regions of interest. Ultra-thin sections were then collected, mounted on formvar-covered copper grids, and stained with uranyl acetate and lead citrate. The sections were examined and photographed in a transmission electron microscope (JEOL 1230).

3.3 COCHLEAR MORPHOMETRIC ANALYSIS

All morphometric analyses were performed on the light micrograph images using SigmaScan Pro 4 Image Analysis software.

3.3.1 Cochlear dimension measurements

Different cochlear parameters were measured on one midmodiolar JB4 section from each group of young (5-9 weeks of age) wild-type (+/+, n=6) and homozygous (*gw/gw*, n=6) animals. The following cochlear parameters were measured inside the bony capsule (Fig. 10): #1, total height of the cochlea from the apical to basal turn; #2, cross-sectional area of the cochlea; #3, the width of the cochlea at the second turn between left and right lateral walls; #4, cross-sectional area of the fluid compartments at the second turn. The parameters for stria vascularis and spiral ligament were measured at the second cochlear turn: #5, the height of stria vascularis; #6, the width of stria vascularis at its mid-height; #7, the height of spiral ligament; #8, the width of spiral ligament at its mid-height; #9, the width of spiral ligament between stria vascularis at its mid-height and the lateral wall; #10, cross-sectional area of the spiral ligament.

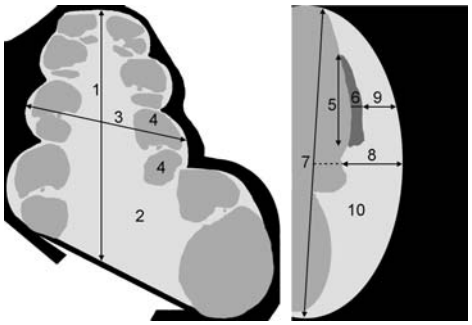

Figure 10. Schematic illustration showing the measurements of different cochlear parameters (paper I).

3.3.2 Spiral ganglion neuron profile density

To compare the size of spiral ganglion neuron (SGN) population in different animal groups, SGN profile density was estimated within Rosenthal's canal. The number of SGN (both type I and II) with a clear nuclear profile and the cross-sectional area of Rosenthal's canal were measured at two locations separated by a half turn on both sides in the first, second and third cochlear turn on six consecutive cochlear midmodiolar sections. The SGN profile density within Rosenthal's canal was represented as SGN number divided by the cross-sectional area of Rosenthal's canal. SGN profile densities from five groups of animals were compared: young adult (5-9 weeks of age) +/+, n=9; young adult *gw*/+, n=6; young adult *gw/gw*, n=6; old +/+ (1-2 years of age), n=2; old *gw/gw*, n=7.

3.4 MOLECULAR BIOLOGY TECHNIQUES

3.4.1 Total RNA isolation

Whole cochleas or micro-dissected cochlear lateral wall/stria vascularis tissues were immediately homogenized with a plastic pestle in TRIzol solution (Invitrogen) or RLT lysis buffer contained in RNeasy Micro Kit (Qiagen). The tissue lysates were further passed through a 20-gauge needle attached to a sterile syringe several times until a homogenous lysate was achieved. Total RNA isolation was subsequently performed following TRIzol or RNeasy Micro Kit protocols. The isolated total RNA was cleaned up with RNeasy MinElute spin column (Qiagen) and subjected to on-column DNase I digestion (Qiagen) to minimize potential DNA contamination. The concentration and integrity of total RNA was determined using the RNA 6000 Nano assay on an Agilent 2000 Bioanalyzer (Agilent Tech). Only RNA sample with a 28S/18S rRNA ratio more than 1.0 was used for RT-PCR experiment (Fig. 11).

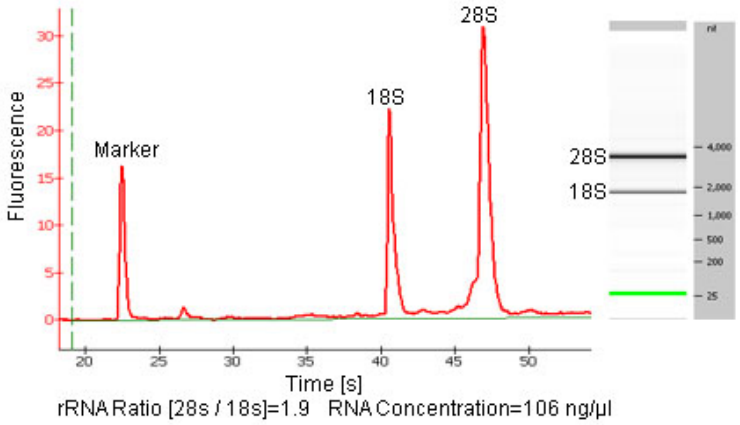

Figure 11. Representative electropherogram and gel-like image showing total RNA preparation with high quality (28S/18S rRNA ratio≥1).

3.4.2 Semi-quantitative RT-PCR

Due to its convenience and high reproducibility, single step RT-PCR was used in the present study. RT-PCR was performed using SuperScript ™ One-Step RT-PCR with Platinum® *Taq* System (Invitrogen). Guinea pig gene-specific primer pairs were either retrieved from published papers or designed from highly conserved region of human/mouse/rat sequences with online Primer 3 primer design tool

(http://frodo.wi.mit.edu/cgi-bin/primer3/primer3_www.cgi). Primer sequences are listed in table 5.

Table 5. PCR primer sequences

Gene	Primer sequence (5'-3') *f*-forward primer, *r*- reverse primer	Product size (bp)	Annealing temperature (ºC)
Pax3	*f*-CGTGCCGTCAGTGAGTTCCA *r*-CGCTTTCCTCTGCCTCCTTC	101	60
Sox10	*f*- AGGTGCTCAGCGGCTACGA *r*- TTGGGCGGCAGGTAYTGGTC	679	55
Edn3	*f*- CAGGATTCGTGCCTTGCTC *r*- CCGTCTGTTCGGGAGTGTT	324	50
Kitl	*f*- GATCTGCGGGAATCCTGTGA *r*-CGGCGACATAGTTGAGGGTTA	98	50
Kit	*f*- CCCACCCTGGTCATTACAGA *r*- CCGICCITGAGTRAGGAGGA	420	56
Mitf	*f*- CCCAACGGCAGCAGGTAAA *r*- CAGGACGCTCGTGAATGTG	259	55
Dct	*f*- GATTAGTCGGAACTCRAGATT *r*- CATTAGTCACYGGWGGGAAG	509	49
Cldn11	*f*- GACCACCTCCACCAATGACT *r*- CCCGCAGTGTAGTAGAAACG	516	55
Kcnj10	*f*- CCTCATTGGCTGCCAGGTGACA *r*- TGCCTTCCTTTTCAGCTTGCTC	487	56
Kcnq1	*f*- GGATGGAGATTGTCCTGGTG *r*- CCTGGCGATGGATGAAGA	309	62
Atp1a1	*f*- AGCGATTCTTTGTTTCTTGG *r*- CACCAGTGAGCGAGGAGTTA	341	50
Atp1b2	*f*- TATCCTCCTCTTCTACCTCGT *r*- GGGCTTGGATAGAGTCGTT	254	50
Slc12a2	*f*- GGAATGGAGTGGGAAGCA *r*- CTTTGGGTATGGCTGACTGA	283	53
Gjb2	*f*- TCCCCATCTCBCACATCCGGC *r*-AAGATGACCCGGAAGAAGATRCTG	232	58
Gjb6	*f*- GAAGCAGCCTTTATGTATGTGT *r*- AGCAGCAGGTAGCACAACTC	206	50
Gjb3	*f*- ACGAGCAAAAAGACTTTGACT *r*- ATCCTGTGGAAGATGAGGTAG	505	53
Gapdh	*f*- GCCAACATCAAGTGGGGTGATG *r*- GTCTTCTGGGTGGCAGTGATG	310	60

The contents of a 25-µl RT-PCR reaction were: 12.5 µl of 2× reaction mix [containing 0.4 mM of each deoxynucleotide triphosphate (dNTP), 2.4 mM $MgSO_4$], 50 ng of total RNA, 0.5 µl each of forward and reverse primers (10 µM), and 0.5 µl of RT/Platinum® *Taq* enzyme mix. The optimal annealing temperature and PCR cycle number of each primer pair were determined with a gradient thermocycler (PTC-200, MJ research). The following thermal cycling conditions were used: reverse transcription at 45-55ºC for 30 minutes, pre-denaturation at 94ºC for 2 minutes, followed by optimal cycle of denaturation at 94ºC for 15 s, annealing at 49-62ºC for 30 s, extension at 72ºC for 1 minute, and a final extension at 72ºC for 10 minutes. Glyceraldehyde-3-phosphate dehydrogenase (*Gapdh*) was run as a positive control for each RNA template. A negative control omitting RNA template from reaction was carried out to detect any DNA contamination in the reaction. Absence of genomic DNA in the RNA template was further verified by omitting the RT/Platinum® *Taq* mix and substituting with 2 units of Platinum® *Taq* DNA polymerase (Invitrogen). The RT-PCR condition has

been optimized to yield PCR products within a linear amplification range in order to compare the relative gene expression. Triplicate RT-PCR amplifications were performed from each RNA template. PCR products were electrophoresed on 2% agarose gels containing ethidium bromide (0.5 μg/ml), and visualized under UV light. PCR products were directly sequenced after gel extraction with QIAquick Gel Extraction Kit (Qiagen), using DYEnamic ET terminator cycle sequencing kit (AmershamPharmacia Biotech), and an ABI100 model 377 sequencer (KIseq, the DNA sequencing core at Karolinska Institutet).

3.5 IMMUNOHISTOCHEMISTRY

To prepare cryosections, decalcified cochleas were washed with 0.1 M PBS several times and immersed in 30% sucrose overnight for cryprotection. The cryoprotected cochleas were embedded in O.C.T. compound (Sakura Tissue-Tek), snap frozen in dry ice with isopentan. Cochlear cryosections were cut at 12-μm thickness in a cryostat (Leica) and mounted onto poly-D-lysin-coated SuperFrost glass slides (Erie Scientific). Selected cryosections were re-hydrated in 0.1 M PBS before the immunostaining, whereas whole-mount cochlea and flat-mount cochlear lateral wall/stria vascularis were directly processed for immunohistochemical labeling.

For immunoperoxidase staining, the tissues were pretreated with 0.3% H_2O_2 for 10 minutes to inactivate the endogenous peroxidase activity. All tissues were incubated with a blocking solution (containing 3-10% normal goat serum, 0.1-0.3% Triton X-100 in 0.1 M PBS) for 1 h at room temperature, followed by incubation with primary antibodies (listed in table 6) at 4ºC overnight. Two different visualization approaches were used: (1) fluorophore-conjugated secondary antibodies (table 6) for 1 h at room temperature; (2) Avidin: Biotinylated enzyme complex (ABC) approach using biontinylated secondary antibodies (table 6), avidin-biotin-peroxidase complex, and peroxidase substrate (e.g. VIP from Vector Lab). In order to evaluate the antibody specificity, negative controls reactions were performed in parallel, by pre-absorption of the primary antibody with excess control antigen peptide, or by omission of primary or secondary secondary antibodies. The immunolabelling reactions were observed and documented under a stereomicroscope (Leica), a light microscope (Zeiss), a fluorescence microscope (Zeiss), or a confocal laser scanning microscope system (Zeiss LSM 510).

Table 6. Primary and secondary antibodies used for immunohistochemistry.

Antibody	Mono/poly clonal	Host	Concentration	Producer	Paper
Primary					
Anti-myosin VIIa	Polyclonal	Rabbit	1:1000	Dr. Tama Hasson, USA	II
Anti-NF-L	Monoclonal	Mouse	1:200	Santa Cruz	II
Anti-KCNJ10	Polyclonal	Rabbit	1:100/400	Alomone	III, IV
Anti-TUJ1	Monoclonal	Mouse	1:250	Covance	III
Anti-KCNQ1	Polyclonal	Rabbit	1:800	Chemicon	IV
Anti-connexin 26	Polyclonal	Rabbit	1:250	Dr. David Kelsell, UK	IV
Anti-SLC12A2	Monoclonal	Mouse	1:200	Iowa hybridoma bank	IV
Anti-claudin 11	Monoclonal	Mouse	1:1	Dr. Alexander Gow, USA	IV
Secondary					
Cy3-anti-rabbit IgG	Polyclonal	Goat	1:2000	Jackson ImmunnoLab	II-IV
FITC-anti-mouse IgG	Polyclonal	Goat	1:400	Jackson ImmunnoLab	II-IV
Alexa 594-anti-mouse IgG2A	Polyclonal	Goat	1:600	MolecularProbes	IV
Alexa 488-anti-mouse IgG	Polyclonal	Goat	1:500	MolecularProbes	IV
Biotinylated anti-rabbit IgG	Polyclonal	Goat	1:1000	Vector Lab	III
Biotinylated anti-mouse IgG	Polyclonal	Goat	1:1000	Vector Lab	IV

3.6 APOPTOSIS DETECTION TUNEL ASSAY

Cochlear cryosections were prepared for terminal transferase dUTP nick end labeling (TUNEL) assay. The TUNEL assay is a common method to detect apoptosis-induced DNA fragmentation. In the present study, it was performed using ApopTag Plus peroxidase *in situ* apoptosis detection kit (Chemicon) following the manufacturer's instruction. In brief, sections were post-fixed in ethanol: acetic acid (2:1) for 5 minutes at -20ºC. Endogenous peroxidase was then quenched in 3% hydrogen peroxide in PBS for 5 minutes at room temperature (RT). After incubation with terminal deoxynucleotidyl transferase (TdT) enzyme in a humidified chamber for 1 h at 37°C followed by anti–digoxigenin peroxidase conjugate for 30 minutes at RT, sections were developed with diaminobenzidine (DAB) substrate for 3 minutes at RT and counterstained in methyl green solution (Vector Lab) for 1 minute at 60ºC. Sections were examined under a light microscope (Zeiss). Substitution of TdT enzyme with distilled water was used as negative control. Slides containing normal female rodent mammary gland tissue (1-2% of the total number of cells on the slide are apoptotic) served as positive controls.

3.7 BIOTIN TRACER PEMEABILITY ASSAY

Guinea pigs (+/+, *gw/+* and *gw/gw*) were anesthetized with an overdose pentobarbital and transcardially perfused with 0.9% saline to flush out blood cells. The cocheas were dissected out and both the round and oval windows were opened in 0.1 M PBS containing 1 mM $CaCl_2$. About 500 µl 10 mg/ml EZ-Link^{TM} Sulfo-NHS-LC-Biotin (Pierce Chemical) were perilymphatically perfused into the cochleas for 10 minutes followed by washing 5 times with 0.1 M PBS containing 1 mM $CaCl_2$. The cochleas were fixed with 10% TCA (Sigma) for 2 hours and further processed for cryosection. In order to visualize the distribution of the biotin tracer, the cryosections were incubated with streptavidin/fluorescein-isothiocyanate (FITC) (1:500, R&D) for 15 minutes and washed several times with 0.1 M PBS. Slides were examined under a fluorescence microscope (Zeiss).

3.8 STATISTICAL ANALYSIS

One-way ANOVA was used for comparison of spiral ganglion cell profile density as well as cochlear parameter measurements. The level of significant statistical difference was set at $p<0.001$. Statistical analysis was performed with the Origin 6.0 program.

4 RESULTS

As the first step towards identification of the molecular substrate causing deafness in the German waltzing guinea pig inner ear, the cochlear morphology and its dynamic alteration during development were presented in this thesis. Based on the results from the cochlear phenotype study, a series of candidate genes were selected. The expression of these candidate genes and proteins was further investigated in the homozygous German waltzing guinea pig (*gw/gw*). The wild-type (+/+) and heterozygous (*gw*/+) animals served as control for comparison.

4.1 COCHLEAR MORPHOLOGY OF THE GERMAN WALTZING GUINEA PIG (*GW/GW*)

4.1.1 Whole cochlea gross morphology

In many deaf mouse mutants, malformed cochleas are usually caused by morphogenetic defects in the inner ear. In paper I, cleared cochleas from neonatal +/+, *gw*/+, and *gw/gw* animals were prepared for gross morphology examination. The external feature of whole cochlea from *gw/gw* animals resembled to that from +/+ and *gw*/+, excepting the appearance of the pigmented stria vascularis. It appeared thinner and contained less pigment in the apical turn, compared to that of +/+ and *gw*/+ animals. Flat-mount cochlear lateral wall preparations showed the presence of large dendritic cells containing unevenly clustered pigments along the *gw/gw* stria vascularis. The pigment was identified as melanin bleached by diluted hydrogen peroxide. The above data suggest that the pigmented melanocyte in the *gw/gw* stria vascularis might be affected.

4.1.2 Progressively diminished scala media

In paper I and II, midmodiolar cross-sections through the JB4-embedded cochlea from the +/+ and *gw/gw* animals at different ages were examined under a light microscope.

In the +/+ embryos/animals, the volume of the scala media steadily increased from embryonic day (E) 25 to E60, and remained constant after birth. The shape of scala media was oval at E25, and transformed to triangular from E30. At E35, the Reissner's membrane containing two cell layers developed and separated the scala vestibuli from the scala media; the pigmented stria vascularis thickened and was distinctive from the adjacent spiral ligament; the amorphous tectorial membrane covered the greater epithelial ridge. The formation of the inner spiral sulcus space and triangular tunnel of Corti was observed from E45 and E50, respectively. The general structure within the scala media displayed adult-like pattern from E60.

In contrast, in the *gw/gw* embryos, the scala media gradually reduced from E35 to E45, and was completely lost from E50 and onwards, due to the depression of the Reissner's membrane. The degree of reduction was similar at different turns along the cochlear spiral. At E40, the Reissner's membrane started to fall and attach with the tectorial membrane. The inner spiral sulcus space was still present at E45 but was filled with severely deformed tectorial membrane from E50. A complete collapse of the Reissner's membrane onto the organ of Corti and stria vascularis was observed from E50 in most

of the *gw/gw* embryos, although it appeared structurally intact and had no visible ruptures. However, in a few of older embryos (older than E50) and younger postnatal animals (5-9 weeks of age), the membrane was not always fully collapsed, leaving a small "scala media" over the outer sulcus cells and the spiral prominence. These scala media remnants could be found in any of the cochlear turns.

Morphometric measurements (cf. Fig. 10) in the cochleas from young +/+ and *gw/gw* animals (5-9 weeks of age) showed no differences in cochlear height from base to apex (#1), total cochlear cross-sectional area inside the bone (#2) and width at each cochlear turn (#3), nor did the cross-sectional area of cochlear fluid compartments (#4) differ.

The progressive reduction of the scala media compartment in the *gw/gw* cochleas indicates the production of endolymph and cochlear fluid homeostasis might be interrupted.

4.1.3 Stria vascularis dysplasia and abnormal melanocyte

Stria vascularis plays an essential role in maintaining cochlear fluidic and ionic homeostasis. The defect in the stria vascularis leads to the enlargement or reduction of the cochlear duct. In paper I and II, the pathological alterations in the *gw/gw* stria vascularis were analyzed in detail by light microscopy and transmission electron microscopy.

In the +/+ embryos, the primordial stria vascularis were first visible on the cochlear lateral wall at E25. It comprised two layers of oval cells and was separated from the underlying mesenchymal cells by an intact basal lamina. At E30, the basal lamina began to fragment while the pigment cells (future intermediate cells) still resided in the mesenchyme. At E35, at least marginal cells and pigmented intermediate cells could be identified in the stria vascularis. The basal lamina under the marginal cell layer was almost fully degraded. The marginal cells were coupled by tight junctions; their apical membrane contained numerous microvilli and oval vesicles, but their basal membrane processes were barely developed. Round-shaped intermediate cells contained a moderate number of evenly distributed melanosomes, and they already had direct contact with marginal cells. Basal cells were not easily distinguished from the mesenchymal cells in the spiral ligament at this stage. At E35, the marginal cells extended their basal cytoplasmic membrane and encircled the intermediate cells, which had increasing number of melanosomes. The spindle-shaped basal cells commenced to orient tangentially in parallel with the surface of the developing stria vascularis, and formed a distinct layer underneath the intermediate cells. At E45, the marginal cells further developed their basolateral processes, but the small vesicles disappeared from the apical membrane. Blood vessels, more intermediate and basal cells were incorporated in the stria vascularis. The stria vascularis attained the adult-like structure from E50. The three characteristic cell layers built an intricate network: the marginal cells containing many mitochondria extended their well-developed basolateral infoldings downward to the basal cells; the basal cells formed a continuous barrier separating them from the adjacent spiral ligament; the pigmented intermediate cells as well as blood capillaries were distributed in between. The height of the stria vascularis gradually increased from E35 to E60 and it appeared more compact over time.

In contrast, in the *gw/gw* cochlea, the stria vascularis was much shorter and thinner than that in the +/+ cochlea at any stage from E35 till adulthood. At E25 and E30, the

morphology of the stria vascularis was not distinguished from the +/+ embryo. However, the *gw/gw* stria vascularis was overall underdeveloped from E35. It consisted of only one marginal cell layer, which was separated by a partially degraded basal lamina. The columnar-shaped marginal cells had rather flat basolateral membranes, and did not contain microvilli and oval vesicles in the apical membrane. Only a few pigmented intermediate cells and mesenchymal cells within the spiral ligament had contacts with the marginal cells. At E40, the stria vascularis appeared extremely disorganized and less compact. Enlarged intercellular spaces existed between the underdeveloped marginal cells. The intermediate cells scattered within the spiral ligament and showed signs of degeneration: cytoplasm shrinkage and nucleus condensation. The typical basal cells were not easily recognized. At E45, large empty spaces were present between and under the marginal cells. Only a few degenerated intermediate cells could be observed beneath the marginal cells in spite of no direct contact between them. At E50, the intact Reissner's membrane collapsed onto the apical surface of the marginal cells, leaving a narrow space in between. The cuboidal marginal cells did not display the typical mitochondria-rich basolateral infoldings observed in the +/+ stria vascularis. They were coupled by tight junctions and formed the only identifiable cell layer in the *gw/gw* stria vascularis. A few degenerated intermediate cells with melanosomes accumulation scattered under the marginal cell layer as well as within the spiral ligament. The basal cells were still not identifiable. From E60 and onwards, the stria vascularis pathology appeared very similar to that observed at E50.

Morphometric analysis (cf. Fig. 10) showed that the height (#5) and width (#6) of stria vascularis at each cochlear turn in the young *gw/gw* animals (5-9 weeks of age) were only 33% and 17% of that in the +/+ animals, respectively. For spiral ligament, height (#7), width at its mid-height (#8) or cross-sectional area (#10) did not differ between groups, however, its width at the mid-height level of stria vascularis (#9) in the *gw/gw* animals was significantly different from that in the +/+ animals.

The TUNEL assay performed on the cochlear cryosections did not detect any apoptotic cells in the *gw/gw* stria vascularis and spiral ligament at any examined stage including postnatal ages.

Our data suggest that the stria vascularis is the primary defect site in the German waltzing guinea pig cochlea. Deficient and abnormal intermediate cells (melanocytes) are responsible for the stria vascularis dysplasia.

4.1.4 Secondary degeneration of sensory hair cells

Prior to embryonic day E50, the morphology of the sensory epithelium in the *gw/gw* cochlea resembled to that in the +/+ cochlea. Amorphous tectorial membranes appeared from E30, and sensory hair cells could be distinguished from surrounding supporting cells from E35. At E50, variable degeneration and loss of sensory hair cells were manifested in the *gw/gw* cochlea when the Reissner's membrane fully collapsed onto the organ of Corti. The inner spiral sulcus was filled with a severely deformed tectorial membrane, but the tunnel of Corti and space of Nuel were still present. Expression of Myosin VIIA, a hair cell-specific marker, was normal from E35 to E45, but it was absent due to the variable loss of hair cells from E50. From E60 and onwards, the degeneration of the sensory epithelium proceeded. The extent varied among different individuals: some hair cells had regular shape, intact cuticular plates,

tight junctions, and nerve endings, whereas others were missing and replaced by scar tissue.

4.1.5 Loss of spiral ganglion neuron

The morphology of spiral ganglion neurons in the *gw/gw* embryos/animals was quite similar to that in the +/+ and *gw/+* embryos/animals from prenatal stages to 5-9 weeks of age after birth. It was also evidenced by constant expression of a neuronal marker neurofilament in the spiral ganglion neuron somata and their dendritic processes of *gw/gw* embryos/animals.

The spiral ganglion profile density was calculated and compared in several postnatal animal groups. Neither the *gw/+* nor the *gw/gw* animal groups differed in spiral ganglion profile density compared with the +/+ animal group at 5-9 weeks of age. The profile density was only slightly lower (7%) in the old +/+ animal (1-2 years of age). However, in the old *gw/gw* animal, the cell profile density was significantly lower (38%). The above findings indicate a dramatic loss of spiral ganglion neurons in the old *gw/gw* animal.

4.2 DIFFERENTIAL EXPRESSION OF KEY CANDIDATES IN THE GW/GW COCHLEA

4.2.1 Ion transport and homeostasis related genes/proteins

On the basis of the above histological findings, it is presumed that the cochlear fluid and ion homeostasis are severely disrupted in the German waltzing guinea pig inner ear. Therefore, the cochlear expression of one group of candidate genes which are key regulators in the cochlear ion (particularly K^+) transport pathway was chosen to investigate further.

The developmental expression and localization of the potassium channel KCNJ10 was first studied in the cochlea of normal guinea pigs. Weak expression of *Kcnj10* mRNA was detected in the cochlea from E30 to E40. Moderate expression was observed at E45, increased rapidly at E50, and remained stable into adulthood. KCNJ10 immunoactivity was first observed in the myelin sheath around cochlear nerve fibers at E40. Only a few satellite cells in the basal turn displayed KCNJ10 immunoactivity. At E45, KCNJ10 staining in the spiral ganglion satellite cells of the basal turn preceded that of the apical turn, displaying a base-to-apex gradient. From E50 and onwards, KCNJ10 labelling was detected in the strial intermediate cells, spiral ganglion satellite cells, and supporting cells in the organ of Corti at each cochlear turn.

Semi-quantitative RT-PCR analysis showed that expression of the tight junction gene *Cldn11* was markedly decreased in both E40 and adult *gw/gw* cochlear lateral wall tissue. The gap junction gene *Gjb2* mRNA expression was reduced at E40 but regained to normal levels at adulthood in the *gw/gw* cochlear lateral wall tissue. No expression of *Kcnj10* was detected in E40 cochlear lateral wall tissue, whereas it was expressed at a relatively equal level in the adult +/+ and *gw/gw* cochlear lateral wall. Expression of mRNA transcripts for the potassium gene *Kcnq1*, gap junction genes *Gjb3* and *Gjb6*, ATPase subunit genes *Atp1a1* and *Atp1b2*, and the Na-K-Cl cotransporter gene *Slc12a2*

were not significantly changed in either E40 or adult +/+ and *gw/gw* cochlear lateral wall tissue.

Flat-mount cochlear lateral wall immunolabelling showed complete loss of KCNJ10 in the intermediate cells and CLDN11 in the basal cells, weak and diffused staining of KCNQ1 in the marginal cells of adult *gw/gw* animals. Immmunohistochemistry on the cochlear cryosections revealed the absence of CLDN11 from E40 and absence of KCNJ10 as well as SLC12A2 from E50 in the gw/gw stria vascularis, but they were still present in the other cochlear structures. KCNQ1 immunoreactivity was first detected in the apical membrane of marginal cells in both +/+ and *gw/gw* stria vascularis at E35. Its expression persisted to adulthood, although it seemed weaker than that in the corresponding +/+ stria vascularis. Gap junction GJB2 was lost between strial basal cells but present between outer sulcus cells from E40 and onwards in the *gw/gw* cochlea. GJB2 immunoreactivity between fibrocytes was temporarily lost at E50, but recovered from E60 until adulthood in the *gw/gw* cochlea.

4.2.2 Strial melanocyte development related genes

Since the intermediate cells (neural crest-derived melanocytes) within the gw/gw cochlear lateral wall appeared degenerated and existed in an insufficient number, the other group of candidate genes encoding for melanocyte-specific marker and melanocyte development regulators was studied further.

RT-PCR analysis showed that the expression of the melanocyte marker gene *Dct* and transcription factor gene *Pax3* was dramatically decreased in both E40 and adult *gw/gw* cochlear lateral wall tissue. However, there was no reduction of *Pax3* transcript in the adult *gw/gw* skin and diaphragm muscle. Expression of other melanocyte development regulator genes such as *Sox10*, *Edn3*, *Kitl*, *Kit* and *Mitf* was not apparently changed in the *gw/gw* cochlear lateral wall tissue.

4.3 ABSENCE OF A STRIAL BASAL CELL BARRIER IN THE GW/GW COCHLEA

A Biotin tracer permeability assay showed that in the neonatal *gw/+* and +/+ cochlear lateral wall, the biotin reagent freely diffused within the spiral ligament, but did not enter the intrastrial compartment. In contrast, the biotin reagent was distributed both under marginal cell layer and within the spiral ligament in the *gw/gw* cochlea, indicating incompletely sealed intrastrial compartment.

5 DISCUSSION

The German waltzing guinea pig is a novel strain of animals with recessive hereditary deafness and a distinct inner ear defect. The pre- and postnatal cochlear pathology in the homozygous German waltzing guinea pig (*gw/gw*) was described in this study, with a focus on the cochlear secretory epithelium-stria vascularis. In addition, the possible molecular mechanism underlying this specific auditory defect was also investigated here. The following aspects are of particular interests and will be discussed in detail.

5.1 A NEW DEAF ANIMAL MUTANT WITH COCHLEOSACCULAR DEFECT

As determined by systematical breeding, the hearing loss in the German waltzing guinea pig is inherited as an autosomal recessive trait. The homozygous animals (*gw/gw*) are deaf already at birth and display a waltzing behavior throughout life; the heterozygous animals (*gw/+*) do not suffer from hearing loss and vestibular symptom.

.

In paper I, morphological analysis of the cochlea in postnatal *gw/gw* animals revealed a collapse of scala media, atrophy of stria vascularis, and degeneration of sensory hair cells and spiral ganglion neurons. This cochlear pathology is reminiscent of what has been described in other animal mutants with cochleosaccular defects, as well as in human temporal bone specimens with Scheibe's type dysplasia (cf. table 2 in paper I). The observation that the earliest cochlear pathology occurred in the stria vascularis of the *gw/gw* embryos further indicates a primary stria vascularis defect, the main feature of a cochleosaccular defect. However, cochlear phenotype differs in the following aspects between the *gw/gw* and above mentioned animal mutants. 1) Time of occurrence of the initial falling of Reissner's membrane and subsequent reduction of the scala media. In the *gw/gw* cochlea, these pathological changes appeared as early as embryonic day (E) 35. In contrast, these abnormalities first arise postnatally in the other animal mutants with cochleosaccular defects. For example, in the cochlea of *Kcnq1*-null mice these occurred from postnatal day (P) 3 (Casimiro et al. 2001). The time difference could be partially explained by the fact that guinea pigs inner ear fully develops already in utero, whereas in the altricial species (e.g. mice, dogs, and cats) a substantial amount of inner ear development occurs after birth (Mullen et al. 2004). 2) Coincidence between reduction/collapse of the scala media and dysplasia/degeneration of the stria vascularis. Without exception, both pathological alterations were simultaneously observed in the *gw/gw* cochlea. However, it does not always happen in the other animal mutants with cochleosaccular defects. For instance, in the cochlea of microphthalmia (mi^{bw}/mi^{bw}) mice the abnormally thin stria vascularis lacked melanocytes despite the present of intact scala media (Motohashi et al. 1994). 3) Stria vascularis pathology at different cochlear turn. Dysplasia of the stria vascularis in the *gw/gw* cochlea was similar along the cochlear spiral without any observed longitudinal gradient. By contrast, in some animal mutants the stria vascularis pathology displays a distinct turn-dependent difference. As an example, in the white spotting (*W*s) rats the stria vascularis appeared normal in the lower turn but severely degenerated in the upper turn (Hoshino et al. 2000).

Scheibe's type inner ear deformity is more frequently observed in temporal bones of patients with syndrome deafness (e.g. Waardenburg syndrome), but it is rarely associated with non-syndromic deafness. The German waltzing guinea pigs have normal coat color and fertility. Although a detailed study on the *gw/gw* vestibular pathology has not been undertaken, our preliminary data showed a similar collapse of saccular wall and loss of pigmentation in the vestibular epithelium (unpublished data). By far, the abnormality is limited to the inner ear of the German waltzing guinea pig, but not other organs we have examined (retina and kidney). Thus, it is currently considered as a good animal model for human non-syndromic deafness.

The degeneration of sensory hair cells in the *gw/gw* cochlea was first observed at E50, which occurred much later than stria vascularis dysplasia, indicating the degeneration is secondary to stria vascularis defect. The degree of hair cell degeneration varies among individual animals, even at the same stage/age. Although in neonatal and young *gw/gw* animals, hair cells and the nerve endings beneath them were usually present, it seemed to degenerate with increasing age. The spiral ganglion cell profile density in young *gw/gw* animals (5-9 weeks of age) did not differ from that in age-matched *gw/+* animals, but there was a significant reduction in old *gw/gw* animals (1-2 years of age). The loss of spiral ganglion neurons over time is not solely attributed to aging factors, since it was far less obvious in age-matched senescent *gw/+* animals. In despite of the large time span within groups (4 weeks in young animal groups and 1 year in old animal groups), the variance is quite low and it is feasible to assume the degeneration of spiral ganglion neurons in the *gw/gw* cochlea is a dynamic and slower process, in contrast to that observed in experimentally evoked deafness (e.g. Shinohara et al. 2002). However, future investigations recruiting several age groups (between 5-9 weeks and 1-2 years of age) are required to elucidate the detailed temporal and spatial degenerations of hair cells and spiral ganglion neurons in the German waltzing guinea pig. Slow retrograde degeneration of spiral ganglion neurons has also been reported in other animal mutants with inherited deafness, such as the NIH strain of waltzing guinea pig (Webster and Webster 1981), deaf white cats (Mair 1973) and Dalmatian dogs (Mair 1976). It is well known that the efficacy of cochlear implants in deaf patients is expected to correlate with the number of excitable spiral ganglion neurons. Thus, the young German waltzing guinea pig may be a potentially useful animal model for cochlear implantation and cell/gene therapy.

5.2 STRIA VASCULARIS AND MELANOCYTE

The cochlear secretory epithelium, stria vascularis, has been widely accepted as the main source for the high endolymphatic [K^+] and the EP (Konishi et al. 1978; Tasaki and Spyropoulos 1959). Therefore, normal development of the stria vascularis is required for structural and functional integrity of the cochlea. In the *gw/gw* cochlea, the primordial stria vascularis failed to transform into the highly vascularized multilayered structure. It appeared from E40 as a single epithelium composed of only marginal cells, whileas few melanocytes sparsely scattered in the spiral ligament, and the basal cells were not easily identified. The stria vascularis is atrophic as evidenced by morphometric measurements of strial height and width in the postnatal *gw/gw* animals. The delayed degradation of the basal lamina under the marginal cells layer could interfere with the ion and fluid transport through the stria vascularis. Accumulation of

melanin pigments was observed in the *gw/gw* cochlear lateral wall. Similar observations were also reported in the stria vascularis of chinchilla after exposure to impulse noise (Gratton and Wright 1992), and in light (B^{lt}) mice (Cable et al. 1993) as well as *Slc26a4*-null mice. The underlying mechanism is yet unknown and suffering from free radical damage could be a potential explanation (Wangemann et al. 2004). Although the atrophy of stria vascularis has been extensively described in various deaf animal mutants, such severe degeneration observed in the *gw/gw* stria vascularis has not been previously reported. The morphological analysis suggested that cell death events could occur in the *gw/gw* cochlear lateral wall. In particular, some apoptotic features (e.g. cytoplasm shrinkage and nucleus condensation) were observed in the intermediate cells. Surprisingly, no TUNEL-positive cells were detected in the *gw/gw* cochlear lateral wall, indicating other cell death mechanisms might be involved.

Strial intermediate cells are neural crest-derived melanocytes. Studies of the inner ear in melanocyte-deficient mutant mice suggest that strial melanocytes play essential roles in the proper development of other strial cells as well as generation and maintenance of the EP (Cable et al. 1992; Hoshino et al. 2000; Steel and Barkway 1989). In addition, strial melanocytes may also respond to different auditory stress factors and contribute to changes of hearing function (Barrenäs and Holgers 2000; Bartels et al. 2001). From E35 and onwards, the number of strial melanocytes in the *gw/gw* animals seemed less than that of age-matched +/+ animals, although no quantitative estimation has been attempted in this study. A remarkable reduction of *Dct* (a melanocyte-specific marker) mRNA in both E40 and adult *gw/gw* cochlear lateral wall, further indicates the reduced number of strial melanocytes. The normal skin pigmentation of the German waltzing guinea pig implies that skin melanocytes, which also have neural crest origin, may not be affected. However, we did find many abnormally appearing melanocytes in the *gw/gw* stria vascularis. As noted above, the strial melanocytes displayed signs of degeneration and accumulation of melanosomes. One form of strial melanocytes, the dark melanocytes, which were observed only in adult mice, displayed a similar morphology (Cable and Steel 1991). However, it is as still unclear whether intrinsic molecular elements or local environmental factors within the stria vascularis, or even both, could contribute to the degenerated cell morphology. In the *gw/gw* cochlea, the marginal cells appeared morphologically underdeveloped and/or degenerated, and the basal cells were difficult to identify. It implies that deficient and abnormal melanocytes have severe impacts on the development and interaction of the marginal and basal cells.

A highly connected molecular network, including the genes *Kit*, *Kitl*, *Edn3*, *Ednrb*, *Pax3*, *Sox10* and *Mitf*, regulates the different aspects of strial melanocyte development. Our RT-PCR data revealed that only *Pax3* mRNA transcript was markedly reduced in both E40 and adult *gw/gw* cochlear lateral wall tissue, and slightly decreased in the adult *gw/+* cochlear lateral wall. Interestingly, its expression was normal in adult diaphragm muscle and melanocyte-containing skin tissue. It thus suggests that *Pax3* may not be the primary causative gene; instead some undetermined upstream gene might result in the reduction of *Pax3* gene. We have tested two different antibodies against Pax3 in order to determine its protein expression level. However, these antibodies failed to recognize the antigen peptide of guinea pig Pax3 protein. The *splotch* (*sp*) mouse mutant carries loss-of-function mutations in the *Pax3* gene (Epstein et al. 1991). Homozygous *sp* (*sp/sp*) mice are embryonic lethal and a remarkable

reduction of melanoblasts were observed near the otic vesicle (Hornyak et al. 2001); whereas heterozygous *sp* (*sp/+*) mice survive after birth and show normal auditory function (Steel and Smith 1992). Notably, the heterozygous (*gw/+*) German waltzing guinea pigs also exhibited normal hearing function (Skjönsberg et al. 2005). However, human patients with type I Waardenburg syndrome usually carry heterozygous mutations in the *PAX3* gene and display hearing impairment (Baldwin et al. 1994). The discrepancy of auditory phenotype between mice and humans may be explained by *Pax3/PAX3* gene dosage effects, which are the differences in sufficient Pax3/PAX3 protein amount for normal development of strial melanocytes (Tassabehji et al. 1994). Therefore, we assume that slightly decreased *Pax3* mRNA expression in the *gw/+* cochlear lateral wall might not affect its auditory function.

5.3 KEY PLAYERS IN COCHLEAR FLUID AND ION HOMEOSTASIS

Dysplasia of stria vascularis and the loss of the scala media compartment in the *gw/gw* cochlea imply that cochlear fluid and ion homeostasis are severely disrupted. The high $[K^+]$ and positive EP in the endolymph have been detected in the normal guinea pig cochlea by E49 and 62, respectively (Kanoh et al. 1985; Raphael et al. 1983). Since scala media was collapsed already at E50 in the *gw/gw* cochlea, it is not possible to measure endolymphatic $[K^+]$ and EP, but we could still assume that both of them are most unlikely to develop in the *gw/gw* cochlea.

The establishment of relatively isolated intrastrial compartment as well as the EP generation is dependent on the maturation of intercellular junctions, in particular tight junctions, of strial marginal and basal cells (Souter and Forge 1998). Prior to the formation of high $[K^+]$ in the endolymph, the strial tight junctions have developed (Anniko and Bagger-Sjöbäck 1982). One of the tight junction proteins, CLDN11, is important for the maintenance of EP. *Cldn11*-null mice displayed severe hearing loss and EP depression (Gow et al. 2004; Kitajiri et al. 2004a), although endolymphatic $[K^+]$, scala media compartment, strial marginal cell morphology as well as expression of intercellular junctions, ion channels and pumps remained normal. In the *gw/gw* cochlear lateral wall, both mRNA transcript and protein expression of CLDN11 were markedly reduced and/or absent. In addition, perilymphatically perfused biotin tracer could be detected adjacent to strial marginal cell layer in the *gw/gw* but not +/+ and *gw/+* cochlea. The above findings, together with histological observations, clearly indicate that the functional strial basal cell barrier fails to develop in the *gw/gw* stria vascularis.

The KCNJ10 potassium channel, expressed in the strial intermediate cells, is essential for EP generation and cochlear K^+ homeostasis. Therefore, KCNJ10 channel could be considered as a cellular and functional marker for strial intermediate cells. The persistent expression of the *Kcnj10* mRNA but loss of its protein in the *gw/gw* cochlea suggests the strial intermediate cells remained although they were dysfunctional. Likewise, the differential expression of *Kcnj10* mRNA transcript and protein has been reported in the stria vascularis of *Slc26a4*-null mice despite totally different cochlear morphology. RT-PCR data showed that the expression of *Kcnq1*, *Atp1a1*, *Atp1b2* and *Slc12a2* mRNA transcripts were not significantly changed in the *gw/gw* cochlear lateral

wall. Since *Slc12a2*, *Atp1a1* and *Atp1b2* are present in strial marginal cells as well as in fibrocytes of the spiral ligament, it is still unclear whether these genes are downregulated in strial marginal cells. However, loss of SLC12A2 protein in the *gw/gw* strial marginal cells indicates K^+ uptake function of strial marginal cells was disrupted. The persistent presence of KCNQ1 channel protein in the apical membrane of strial marginal cells in the adult *gw/gw* cochlea, despite at a relatively low level, suggests that K^+ secretion function of strial marginal cells was partially compromised. The temporal loss of gap junction protein GJB2 between spiral ligament fibrocytes in the *gw/gw* cochlea, might be caused by transient inhibition from dysfunctional strial basal/intermediate cells. A recent study reported a *GJB2* mutation associated with cochleosaccular dysplasia in keratitis-ichthyosis-deafness (KID) syndrome by disruption of cochlear epithelial differentiation (Griffith et al. 2006). Therefore, it should be of interest to further investigate the cellular interactions and their molecular correlates in the inner ear, e.g. how strial cells interact with fibrocytes in the spiral ligament by gap junction GJB2.

6 CONCLUSIONS

The German waltzing guinea pig is a new strain of animal mutants with yet unidentified gene mutation(s) displaying recessively inherited cochleovestibular impairment. The homozygous guinea pigs (*gw/gw*) exhibit a severe cochleosaccular defect in the inner ear during embryonic development and thus appear deaf already at birth. Dysplasia of the developing stria vascularis is the primary defect in the cochlea, which causes a progressive collapse of Reissner's membrane and subsequent loss of the scala media compartment. Degeneration of sensory hair cells occurs in a late embryonic stage, and thus results a slow retrograde degeneration of spiral ganglion neurons in the postnatal animals.

The spatial and temporal loss of several key players (KCNJ10, CLDN11 and SLC12A2) in cochlear homeostasis may not be the causative defect, although these changes underlie the malfunction of the strial cells in the *gw/gw* cochlea. Deficient and abnormal strial melanocytes are responsible for the stria vascularis dysplasia. These abnormal melanocytes could migrate to the developing stria vascularis, but fail to provide appropriate support for the subsequent maturation of strial marginal and basal cells, and finally lead to a fully disorganized stria vascularis. Reduction of *Pax3* gene may be involved in the above pathological process, although it is most unlikely to be the primary mutated gene. Dysfunctional strial cells, in particular melanocytes, fail to maintain the integrity of the stria vascularis and eradicate the main cochlear K^+ recycling pathway in the German waltzing guinea pig inner ear, ultimately resulting in the disruption of cochlear homeostasis and cochlear degeneration.

The German waltzing guinea pig is currently considered as a good model for human non-syndromic deafness and may be useful for experimental studies on novel therapeutic strategies.

7 FUTURE PERSPECTIVES

The present work described in the thesis has elucidated that strial intermediate cells (melanocytes) are responsible for the cochlear defect in the German waltzing guinea pig inner ear, although the causative gene has not yet been identified. After years of study, one is tempted to ask whether the old story about the German waltzing guinea pig will eventually have an ending. With the current state of knowledge, several interesting studies can be suggested which might be helpful to answer this question.

Since dopachrome tautomerase (Dct) is a marker for melanoblasts, the approximate number of melanoblasts in the neural crest as well as near the otocyst could be determined in the early *gw/gw* embryo by RNA *in situ* hybridization or immunohistochemistry. This would help to elucidate whether the otic melanoblast population is affected. Another way to evaluate the property of otic melanoblasts or strial melanocytes in the *gw/gw* embryo/animal is to cultivate them *in vitro*. Will these melanoblasts or melanocytes survive and differentiate in the same way as wild-type cells? If not, will electroporation of plasmid containing, for example, normal *Pax3* cDNA to these affected cells change the cell phenotype, "rescue" or revert the deficits observed in *gw/gw* animals? All the above studies, and certainly others, already or yet to be thought up, would be worthwhile to investigate further.

The RT-PCR approach we used in the present study is sensitive and efficient to compare the expression of candidate genes. However, it is only limited to very few genes with known sequence. PCR-based suppression subtractive hybridization (SSH) combined with differential screening has proved to be a more powerful approach in the case of identifying and isolating differentially expressed genes without prior knowledge of nucleotide sequences, for example in a less popular species for molecular studies such as the guinea pig. SSH has been widely used to generate tissue-specific subtracted cDNA libraries and identifying disease-causing genes. Therefore, it is of particular interest to apply this technique to future projects attempting to identify the deafness gene in German waltzing guinea pigs.

Finally, I believe this will be a never-ending story, as the German waltzing guinea pig (and future guinea pig strains?) could serve well as an experimental model to study human genetic deafness, as a means to understand disease mechanisms and eventually developing new (molecular) treatments for hereditary hearing loss.

8 ACKNOWLEDGEMENTS

The work presented in this thesis was performed at the Center for Hearing and Communication Research and the Department of Clinical Neuroscience, Karolinska Institutet and Karolinska University Hospital in Stockholm. I would like to express my sincere gratitude to all those who have directly or indirectly contributed to this work over the past years. In particular, I would like to thank:

Professor Mats Ulfendahl, my supervisor, for providing me the opportunity to be a PhD student and work on such an attracting research project, for leading me into the auditory research field and sharing your extensive scientific knowledge, for supporting me to attend those exciting conferences. As the director of CfH, your brilliant mind, generosity and unexhausted energy deeply impressed me, and thank you for creating such an excellent scientific atmosphere!

Dr. Leif Järlebark, my co-supervisor, for teaching and reinforcing my scientific skills in molecular biology, for being excellent mentor and keeping an eye on the progress of my work, for critical reading and modifying all my abstracts, posters, presentation slides, manuscripts and thesis again and again! I am indebted to you for never getting annoyed by my interruption from time to time. Thank you again for allowing me to work on potassium channel projects when I got stuck in my own project.

Associate Professor MaoLi Duan, my co-supervisor, for introducing and recommending me to study in Sweden, for generously sharing your great knowledge in the auditory field and science in general, for your enthusiastic and valuable advices on my daily life and future career! Your diligence and devotion to science set a great example to me. You are not only a great scientist but also an excellent mentor. I am grateful for your continuous encouragement and support especially during my difficult time.

Professor Malou Hultcrantz, my co-supervisor, for your encouragement and support to my study project. You make me believe that a good surgeon can also be a great scientist.

Professor Åke Flock and **Dr. Anders Fridberger**, for sharing extensive knowledge of neuroscience, particularly auditory neuroscience, for your efforts to organize the Journal Club and create such a wonderful occasion to read and discuss high quality papers.

Associate Professor Ann-Christin Johnson, for encouragement and support during my stay in the lab.

Dr. DongGuang Wei, my co-author, for your true friendship and honesty, for teaching me with cell culture, immunohistochemistry and microscopy techniques, and for our fruitful collaboration. **Dr. GuiHua Liang**, my co-author, for successful collaboration in potassium channel projects.

Dr. Mette Kirkegaard, for enjoyable discussion about molecular biology techniques, for keeping the molecular biology theme group running, for critical reading my manuscripts and valuable comments, for accompanying in the MBHD, IEB and ARO meetings!

The German waltzing guinea pig working group, **Åsa Skjönsberg** and **Paula Mannström**, for such an efficient collaboration and nice discussion on this project. A special thank to Paula, for teaching me histological and Western blot technique, and for taking care of guinea pigs. I am also grateful to **Anette Fransson** for delivering the pregnant guinea pigs to the lab always in time.

Dr. Charoensri Thonabulsombat, for precious friendship, encouragement and beautiful gifts.

Louise von Essen, for administrative and secretarial assistance.

A special thank to **Associate Professor Stefan Ernstson**, for initiating the studies on the German waltzing guinea pig.

My present and past room mates (**Palash, Beata, Shaden, Mette, Miriam, Nathan, JianXin, BuSheng, YongQing, ZhiQiang, Alexandra, YanMing**), for nice chatting and discussion about life and science. **Iram**, **Max** and **Qing**, project students, for sharing the happy time in the lab. All the colleagues, present and past, at the Center for Hearing and Communication Research and ENT clinic, especially **Igor, Qiang, Yen-Fu, Jacques, HongMin, Stefan, Anna E, Hong, Anna M, Martin, Amanj, Eric, Futoshi, Magnus, Björn, Petri, Göran, Cecilia, ZhengQing, Aleksandra,** for making such an active and nice lab.

FuDan University Medical Center, previously ShangHai Medical University in China, for five years medical training. **Associate Professor LiJun Wang**, for continuous encouragement and support over the past five years.

My friends, **JunYong, Xin, and KanLin**, for long-lasting friendship and kind hospitality when we visited Germany.

All the Chinese friends in Stockholm and around the world, in particular present and past members of "Saturday badminton group", **Yan, Bing, Min, Rong, Rui, XiaoFeng, Xin, XiaoWei, JiangNing, JiaYi, Ying, Yu, JiaKun**, for accompanying for the past years and the great time together!

HuaXin Cao, my dear "sister", for your never-ending encouragement and enthusiastic helps and making me always feels at home!

I would like to express my deep gratitude to all my relatives and my beloved family in China. My parents, my first and continuous source of support, strength and inspiration; my sister, who over and over again proves to be the best sister in the world; last but certainly not least, my wife, **QiaoLin**, for your endless love and constant support throughout my life, no matter where I am…

This work was supported by grants from the Swedish Research Council (09888), the Foundation Tysta Skolan, Svenska Sällskapet för Medicinsk Forskning (The Swedish Society for Medical Research), Hörselskadades Riksförbund (The Swedish Association for the Hearing Impaired), Stiftelsen Wenner-Grenska Samfundet, the Swedish Association of Hard of Hearing People (HRF) and the Petrus and Augusta Hedlund Foundation.

9 REFERENCES

Ando M, Takeuchi S. 1999. Immunological identification of an inward rectifier K+ channel (Kir4.1) in the intermediate cell (melanocyte) of the cochlear stria vascularis of gerbils and rats. Cell Tissue Res 298(1):179-183.

Anniko M, Bagger-Sjöbäck D. 1982. Maturation of junctional complexes during embryonic and early postnatal development of inner ear secretory epithelia. Am J Otolaryngol 3(4):242-253.

Araki S, Mizuta K, Takeshita T, Morita H, Mineta H, Hoshino T. 2002. Degeneration of the stria vascularis during development in melanocyte-deficient mutant rats (Ws/Ws rats). Eur Arch Otorhinolaryngol 259(6):309-315.

Baldwin CT, Lipsky NR, Hoth CF, Cohen T, Mamuya W, Milunsky A. 1994. Mutations in PAX3 associated with Waardenburg syndrome type I. Hum Mutat 3(3):205-211.

Barrenäs ML, Holgers KM. 2000. Ototoxic interaction between noise and pheomelanin: distortion product otoacoustic emissions after acoustical trauma in chloroquine-treated red, black, and albino guinea pigs. Audiology 39(5):238-246.

Bartels S, Ito S, Trune DR, Nuttall AL. 2001. Noise-induced hearing loss: the effect of melanin in the stria vascularis. Hear Res 154(1-2):116-123.

Baynash AG, Hosoda K, Giaid A, Richardson JA, Emoto N, Hammer RE, Yanagisawa M. 1994. Interaction of endothelin-3 with endothelin-B receptor is essential for development of epidermal melanocytes and enteric neurons. Cell 79(7):1277-1285.

Békésy G. 1951. DC potentials and energy balance of the cochlear partition. J Acoust Soc Am 22(5):576-582.

Branis M, Burda H. 1985. Inner ear structure in the deaf and normally hearing Dalmatian dog. J Comp Pathol 95(2):295-299.

Buckiova D, Syka J. 2004. Development of the inner ear in Splotch mutant mice. Neuroreport 15(13):2001-2005.

Cable J, Barkway C, Steel KP. 1992. Characteristics of stria vascularis melanocytes of viable dominant spotting (Wv/Wv) mouse mutants. Hear Res 64(1):6-20.

Cable J, Huszar D, Jaenisch R, Steel KP. 1994. Effects of mutations at the W locus (c-kit) on inner ear pigmentation and function in the mouse. Pigment Cell Res 7(1):17-32.

Cable J, Jackson IJ, Steel KP. 1993. Light (Blt), a mutation that causes melanocyte death, affects stria vascularis function in the mouse inner ear. Pigment Cell Res 6(4 Pt 1):215-225.

Cable J, Jackson IJ, Steel KP. 1995. Mutations at the W locus affect survival of neural crest-derived melanocytes in the mouse. Mech Dev 50(2-3):139-150.

Cable J, Steel KP. 1991. Identification of two types of melanocyte within the stria vascularis of the mouse inner ear. Pigment Cell Res 4(2):87-101.

Canlon B, Marklund K, Borg E. 1993. Measures of auditory brain-stem responses, distortion product otoacoustic emissions, hair cell loss, and forward masked tuning curves in the waltzing guinea pig. J Acoust Soc Am 94(6):3232-3243.

Casimiro MC, Knollmann BC, Ebert SN, Vary JC, Jr., Greene AE, Franz MR, Grinberg A, Huang SP, Pfeifer K. 2001. Targeted disruption of the Kcnq1 gene produces a mouse model of Jervell and Lange-Nielsen Syndrome. Proc Natl Acad Sci U S A 98(5):2526-2531.

Chiba T, Marcus DC. 2000. Nonselective cation and BK channels in apical membrane of outer sulcus epithelial cells. J Membr Biol 174(2):167-179.

Cohen-Salmon M, Ott T, Michel V, Hardelin JP, Perfettini I, Eybalin M, Wu T, Marcus DC, Wangemann P, Willecke K, Petit C. 2002. Targeted ablation of connexin26 in the inner ear epithelial gap junction network causes hearing impairment and cell death. Curr Biol 12(13):1106-1111.

Crouch JJ, Sakaguchi N, Lytle C, Schulte BA. 1997. Immunohistochemical localization of the Na-K-Cl co-transporter (NKCC1) in the gerbil inner ear. J Histochem Cytochem 45(6):773-778.
Delpire E, Lu J, England R, Dull C, Thorne T. 1999. Deafness and imbalance associated with inactivation of the secretory Na-K-2Cl co-transporter. Nat Genet 22(2):192-195.
Deol MS. 1970. The relationship between abnormalities of pigmentation and of the inner ear. Proc R Soc Lond B Biol Sci 175(39):201-217.
Dixon MJ, Gazzard J, Chaudhry SS, Sampson N, Schulte BA, Steel KP. 1999. Mutation of the Na-K-Cl co-transporter gene Slc12a2 results in deafness in mice. Hum Mol Genet 8(8):1579-1584.
Engström H, Sjostrand FS, Spoendlin H. 1955. [Fine structure of the stria vascularis in guinea pigs; light and electron microscopical study.]. Pract Otorhinolaryngol (Basel) 17(2):69-79.
Epstein DJ, Vekemans M, Gros P. 1991. Splotch (Sp2H), a mutation affecting development of the mouse neural tube, shows a deletion within the paired homeodomain of Pax-3. Cell 67(4):767-774.
Ernstson S. 1970. Heredity in a strain of the waltzing guinea pig. Acta Otolaryngol 69(5):358-362.
Ernstson S. 1971a. Cochlear morphology in a strain of the waltzing guinea pig. Acta Otolaryngol 71(6):469-482.
Ernstson S. 1971b. Vestibular physiology in a strain of the waltzing guinea pig. Acta Otolaryngol 72(5):303-309.
Ernstson S. 1972. Cochlear physiology and hair cell population in a strain of the waltzing guinea pig. Acta Otolaryngol Suppl 297:1-24.
Ernstson S, Lundquist PG, Wedenberg E, Wersall J. 1969. Morphologic changes in vestibular hair cells in a strain of the waltzing guinea pig. Acta Otolaryngol 67(5):521-534.
Fernandez C, Hinojosa R. 1974. Postnatal development of endocochlear potential and stria vascularis in the cat. Acta Otolaryngol 78(3-4):173-186.
Gow A, Davies C, Southwood CM, Frolenkov G, Chrustowski M, Ng L, Yamauchi D, Marcus DC, Kachar B. 2004. Deafness in Claudin 11-null mice reveals the critical contribution of basal cell tight junctions to stria vascularis function. J Neurosci 24(32):7051-7062.
Gratton MA, Wright CG. 1992. Hyperpigmentation of chinchilla stria vascularis following acoustic trauma. Pigment Cell Res 5(1):30-37.
Griffith AJ, Yang Y, Pryor SP, Park HJ, Jabs EW, Nadol JB, Jr., Russell LJ, Wasserman DI, Richard G, Adams JC, Merchant SN. 2006. Cochleosaccular dysplasia associated with a connexin 26 mutation in keratitis-ichthyosis-deafness syndrome. Laryngoscope 116(8):1404-1408.
Halsey K, Skjönsberg A, Ulfendahl M, Dolan DF. 2005. Efferent-mediated adaptation of the DPOAE as a predictor of aminoglycoside toxicity. Hear Res 201(1-2):99-108.
Heid S, Hartmann R, Klinke R. 1998. A model for prelingual deafness, the congenitally deaf white cat--population statistics and degenerative changes. Hear Res 115(1-2):101-112.
Hibino H, Horio Y, Inanobe A, Doi K, Ito M, Yamada M, Gotow T, Uchiyama Y, Kawamura M, Kubo T, Kurachi Y. 1997. An ATP-dependent inwardly rectifying potassium channel, KAB-2 (Kir4. 1), in cochlear stria vascularis of inner ear: its specific subcellular localization and correlation with the formation of endocochlear potential. J Neurosci 17(12):4711-4721.
Hilding DA, Ginzberg RD. 1977. Pigmentation of the stria vascularis. The contribution of neural crest melanocytes. Acta Otolaryngol 84(1-2):24-37.
Hinojosa R, Rodriguez-Echandia EL. 1966. The fine structure of the stria vascularis of the cat inner ear. Am J Anat 118(2):631-663.
Hodgkinson CA, Moore KJ, Nakayama A, Steingrimsson E, Copeland NG, Jenkins NA, Arnheiter H. 1993. Mutations at the mouse microphthalmia locus are associated with defects in a gene encoding a novel basic-helix-loop-helix-zipper protein. Cell 74(2):395-404.

Hornyak TJ, Hayes DJ, Chiu LY, Ziff EB. 2001. Transcription factors in melanocyte development: distinct roles for Pax-3 and Mitf. Mech Dev 101(1-2):47-59.
Hoshino T, Mizuta K, Gao J, Araki S, Araki K, Takeshita T, Wu R, Morita H. 2000. Cochlear findings in the white spotting (Ws) rat. Hear Res 140(1-2):145-156.
Ibsen L, Risty, T. 1929. A new character in guinea pigs, waltzing. Anat Rec 44:294.
Jin Z, Duan M. 2006. Genetic deafness and gene therapy approaches for treatment. Drug discovery today: Disease mechanisms 3(1):143-150.
Kanoh N, Ohmura M, Fukazawa T, Hirono Y, Makimoto K. 1985. The developing electrolytes concentrations of inner ear fluids in guinea pigs. Acta Otolaryngol 99(5-6):525-528.
Kikuchi K, Hilding DA. 1966. The development of the stria vascularis in the mouse. Acta Otolaryngol 62(4):277-291.
Kikuchi T, Adams JC, Miyabe Y, So E, Kobayashi T. 2000a. Potassium ion recycling pathway via gap junction systems in the mammalian cochlea and its interruption in hereditary nonsyndromic deafness. Med Electron Microsc 33(2):51-56.
Kikuchi T, Kimura RS, Paul DL, Adams JC. 1995. Gap junctions in the rat cochlea: immunohistochemical and ultrastructural analysis. Anat Embryol (Berl) 191(2):101-118.
Kikuchi T, Kimura RS, Paul DL, Takasaka T, Adams JC. 2000b. Gap junction systems in the mammalian cochlea. Brain Res Brain Res Rev 32(1):163-166.
Kimura RS, Schuknecht HF. 1970a. The ultrastructure of the human stria vascularis. I. Acta Otolaryngol 69(6):415-427.
Kimura RS, Schuknecht HF. 1970b. The ultrastructure of the human stria vascularis. II. Acta Otolaryngol 70(5):301-318.
Kitajiri S, Miyamoto T, Mineharu A, Sonoda N, Furuse K, Hata M, Sasaki H, Mori Y, Kubota T, Ito J, Furuse M, Tsukita S. 2004a. Compartmentalization established by claudin-11-based tight junctions in stria vascularis is required for hearing through generation of endocochlear potential. J Cell Sci 117(Pt 21):5087-5096.
Kitajiri SI, Furuse M, Morita K, Saishin-Kiuchi Y, Kido H, Ito J, Tsukita S. 2004b. Expression patterns of claudins, tight junction adhesion molecules, in the inner ear. Hear Res 187(1-2):25-34.
Kitamura K, Sakagami M, Umemoto M, Takeda N, Doi K, Kasugai T, Kitamura Y. 1994. Strial dysfunction in a melanocyte deficient mutant rat (Ws/Ws rat). Acta Otolaryngol 114(2):177-181.
Koide T, Moriwaki K, Uchida K, Mita A, Sagai T, Yonekawa H, Katoh H, Miyashita N, Tsuchiya K, Nielsen TJ, Shiroishi T. 1998. A new inbred strain JF1 established from Japanese fancy mouse carrying the classic piebald allele. Mamm Genome 9(1):15-19.
Konishi T, Hamrick PE, Walsh PJ. 1978. Ion transport in guinea pig cochlea. I. Potassium and sodium transport. Acta Otolaryngol 86(1-2):22-34.
Kros C. 1996. Physiology of mammalian hair cells. In: Dallos P, Popper, A.N., & Fay, R., editor. Handbook of auditory research: The cochlea. New York: Springer. p 319-385.
Kudo T, Kure S, Ikeda K, Xia AP, Katori Y, Suzuki M, Kojima K, Ichinohe A, Suzuki Y, Aoki Y, Kobayashi T, Matsubara Y. 2003. Transgenic expression of a dominant-negative connexin26 causes degeneration of the organ of Corti and non-syndromic deafness. Hum Mol Genet 12(9):995-1004.
Lavigne-Rebillard M, Bagger-Sjöbäck D. 1992. Development of the human stria vascularis. Hear Res 64(1):39-51.
Lee MP, Ravenel JD, Hu RJ, Lustig LR, Tomaselli G, Berger RD, Brandenburg SA, Litzi TJ, Bunton TE, Limb C, Francis H, Gorelikow M, Gu H, Washington K, Argani P, Goldenring JR, Coffey RJ, Feinberg AP. 2000. Targeted disruption of the Kvlqt1 gene causes deafness and gastric hyperplasia in mice. J Clin Invest 106(12):1447-1455.
Letts VA, Valenzuela A, Dunbar C, Zheng QY, Johnson KR, Frankel WN. 2000. A new spontaneous mouse mutation in the Kcne1 gene. Mamm Genome 11(10):831-835.
Lurie MH. 1939. Studies of the waltzing guinea pig. Laryngoscope 49:558.
Lurie MH. 1941. The waltzing (circling) guinea pig. Ann Otol 50:113.
Mair IW. 1973. Hereditary deafness in the white cat. Acta Otolaryngol Suppl 314:1-48.

Mair IW. 1976. Hereditary deafness in the dalmatian dog. Arch Otorhinolaryngol 212(1):1-14.
Marcus DC, Thalmann R. 1980. Comments concerning a possible independent potassium pump in the cochlear duct. Hear Res 2(2):163-165.
Marcus DC, Wu T, Wangemann P, Kofuji P. 2002. KCNJ10 (Kir4.1) potassium channel knockout abolishes endocochlear potential. Am J Physiol Cell Physiol 282(2):C403-407.
Matsushima Y, Shinkai Y, Kobayashi Y, Sakamoto M, Kunieda T, Tachibana M. 2002. A mouse model of Waardenburg syndrome type 4 with a new spontaneous mutation of the endothelin-B receptor gene. Mamm Genome 13(1):30-35.
Mayer TC, Maltby EL. 1964. An Experimental Investigation of Pattern Development in Lethal Spotting and Belted Mouse Embryos. Dev Biol 22:269-286.
Meyer zum Gottesberge AM. 1988. Physiology and pathophysiology of inner ear melanin. Pigment Cell Res 1(4):238-249.
Minowa O, Ikeda K, Sugitani Y, Oshima T, Nakai S, Katori Y, Suzuki M, Furukawa M, Kawase T, Zheng Y, Ogura M, Asada Y, Watanabe K, Yamanaka H, Gotoh S, Nishi-Takeshima M, Sugimoto T, Kikuchi T, Takasaka T, Noda T. 1999. Altered cochlear fibrocytes in a mouse model of DFN3 nonsyndromic deafness. Science 285(5432):1408-1411.
Motohashi H, Hozawa K, Oshima T, Takeuchi T, Takasaka T. 1994. Dysgenesis of melanocytes and cochlear dysfunction in mutant microphthalmia (mi) mice. Hear Res 80(1):10-20.
Mou K, Adamson CL, Davis RL. 1997. Stria vascularis morphogenesis in vitro. Hear Res 103(1-2):47-62.
Mullen L, Li Y, Ryan A. 2004. Normal development of the ear in the human and mouse. In: Willems PJ, editor. Genetic hearing loss. New York: Marcel Dekker. p 1-31.
Neyroud N, Tesson F, Denjoy I, Leibovici M, Donger C, Barhanin J, Faure S, Gary F, Coumel P, Petit C, Schwartz K, Guicheney P. 1997. A novel mutation in the potassium channel gene KVLQT1 causes the Jervell and Lange-Nielsen cardioauditory syndrome. Nat Genet 15(2):186-189.
Nicolas M, Dememes D, Martin A, Kupershmidt S, Barhanin J. 2001. KCNQ1/KCNE1 potassium channels in mammalian vestibular dark cells. Hear Res 153(1-2):132-145.
Offner FF, Dallos P, Cheatham MA. 1987. Positive endocochlear potential: mechanism of production by marginal cells of stria vascularis. Hear Res 29(2-3):117-124.
Ormerod FC. 1960. The pathology of congenital deafness. J Laryngol Otol 74:919-950.
Pace AJ, Madden VJ, Henson OW, Jr., Koller BH, Henson MM. 2001. Ultrastructure of the inner ear of NKCC1-deficient mice. Hear Res 156(1-2):17-30.
Paparella MM, Schachem PA. 1991. Sensorineural hearing loss in children: genetic. In: Paparella MM, Shumrick DA, Gluckman JL, Meyerhoff WL, editors. Otolaryngology. Philadelphia: W.B. Saunders. p 1579-1599.
Pavan WJ, Tilghman SM. 1994. Piebald lethal (sl) acts early to disrupt the development of neural crest-derived melanocytes. Proc Natl Acad Sci U S A 91(15):7159-7163.
Pingault V, Bondurand N, Kuhlbrodt K, Goerich DE, Prehu MO, Puliti A, Herbarth B, Hermans-Borgmeyer I, Legius E, Matthijs G, Amiel J, Lyonnet S, Ceccherini I, Romeo G, Smith JC, Read AP, Wegner M, Goossens M. 1998. SOX10 mutations in patients with Waardenburg-Hirschsprung disease. Nat Genet 18(2):171-173.
Price ER, Fisher DE. 2001. Sensorineural deafness and pigmentation genes: melanocytes and the Mitf transcriptional network. Neuron 30(1):15-18.
Raphael Y, Ohmura M, Kanoh N, Yagi N, Makimoto K. 1983. Prenatal maturation of endocochlear potential and electrolyte composition of inner ear fluids in guinea pigs. Arch Otorhinolaryngol 237(2):147-152.
Read AP, Newton VE. 1997. Waardenburg syndrome. J Med Genet 34(8):656-665.
Rivas A, Francis HW. 2005. Inner ear abnormalities in a Kcnq1 (Kvlqt1) knockout mouse: a model of Jervell and Lange-Nielsen syndrome. Otol Neurotol 26(3):415-424.

Rozengurt N, Lopez I, Chiu CS, Kofuji P, Lester HA, Neusch C. 2003. Time course of inner ear degeneration and deafness in mice lacking the Kir4.1 potassium channel subunit. Hear Res 177(1-2):71-80.
Ryugo DK, Cahill HB, Rose LS, Rosenbaum BT, Schroeder ME, Wright AL. 2003. Separate forms of pathology in the cochlea of congenitally deaf white cats. Hear Res 181(1-2):73-84.
Sakagami M, Fukazawa K, Matsunaga T, Fujita H, Mori N, Takumi T, Ohkubo H, Nakanishi S. 1991. Cellular localization of rat Isk protein in the stria vascularis by immunohistochemical observation. Hear Res 56(1-2):168-172.
Salt AN, Melichar I, Thalmann R. 1987. Mechanisms of endocochlear potential generation by stria vascularis. Laryngoscope 97(8 Pt 1):984-991.
Scheibe A. 1892. A case of deaf-mutism, with auditory atrophy and anomalies of development in the membranous labyrinth of both ears. Arch Otolaryngol 21:12-22.
Schrott A, Melichar I, Popelar J, Syka J. 1990. Deterioration of hearing function in mice with neural crest defect. Hear Res 46(1-2):1-7.
Schulze-Bahr E, Wang Q, Wedekind H, Haverkamp W, Chen Q, Sun Y, Rubie C, Hordt M, Towbin JA, Borggrefe M, Assmann G, Qu X, Somberg JC, Breithardt G, Oberti C, Funke H. 1997. KCNE1 mutations cause jervell and Lange-Nielsen syndrome. Nat Genet 17(3):267-268.
Shinohara T, Bredberg G, Ulfendahl M, Pyykko I, Olivius NP, Kaksonen R, Lindstrom B, Altschuler R, Miller JM. 2002. Neurotrophic factor intervention restores auditory function in deafened animals. Proc Natl Acad Sci U S A 99(3):1657-1660.
Skjönsberg A, Herrlin P, Duan M, Johnson AC, Ulfendahl M. 2005. A guinea pig strain with recessive heredity of deafness, producing normal-hearing heterozygotes with resistance to noise trauma. Audiol Neurootol 10(6):323-330.
Smith CA. 1957. Structure of the stria vascularis and the spiral prominence. Ann Otol Rhinol Laryngol 66(2):521-536.
Sobin A, Weraall J. 1983. A morphological study on vestibular sensory epithelia in a strain of the waltzing guinea pig. Acta Otolaryngol Suppl 396:1-32.
Souter M, Forge A. 1998. Intercellular junctional maturation in the stria vascularis: possible association with onset and rise of endocochlear potential. Hear Res 119(1-2):81-95.
Spicer SS, Schulte BA. 1998. Evidence for a medial K+ recycling pathway from inner hair cells. Hear Res 118(1-2):1-12.
Steel KP. 1995. Inherited hearing defects in mice. Annu Rev Genet 29:675-701.
Steel KP, Barkway C. 1989. Another role for melanocytes: their importance for normal stria vascularis development in the mammalian inner ear. Development 107(3):453-463.
Steel KP, Barkway C, Bock GR. 1987. Strial dysfunction in mice with cochleo-saccular abnormalities. Hear Res 27(1):11-26.
Steel KP, Davidson DR, Jackson IJ. 1992. TRP-2/DT, a new early melanoblast marker, shows that steel growth factor (c-kit ligand) is a survival factor. Development 115(4):1111-1119.
Steel KP, Smith RJ. 1992. Normal hearing in Splotch (Sp/+), the mouse homologue of Waardenburg syndrome type 1. Nat Genet 2(1):75-79.
Sterkers O, Ferrary E, Amiel C. 1988. Production of inner ear fluids. Physiol Rev 68(4):1083-1128.
Sterkers O, Saumon G, Tran Ba Huy P, Amiel C. 1982. K, Cl, and H2O entry in endolymph, perilymph, and cerebrospinal fluid of the rat. Am J Physiol 243(2):F173-180.
Tachibana M. 2001. Cochlear melanocytes and MITF signaling. J Investig Dermatol Symp Proc 6(1):95-98.
Tachibana M, Hara Y, Vyas D, Hodgkinson C, Fex J, Grundfast K, Arnheiter H. 1992. Cochlear Disorder Associated with Melanocyte Anomaly in Mice with a Transgenic Insertional Mutation. Molecular and Cellular Neuroscience 3(5):433-445.
Takeuchi S, Ando M, Kakigi A. 2000. Mechanism generating endocochlear potential: role played by intermediate cells in stria vascularis. Biophys J 79(5):2572-2582.

Tasaki I, Spyropoulos CS. 1959. Stria vascularis as source of endocochlear potential. J Neurophysiol 22(2):149-155.
Tassabehji M, Newton VE, Leverton K, Turnbull K, Seemanova E, Kunze J, Sperling K, Strachan T, Read AP. 1994. PAX3 gene structure and mutations: close analogies between Waardenburg syndrome and the Splotch mouse. Hum Mol Genet 3(7):1069-1074.
Thorn L, Schinko I. 1985. [Light- and electronmicroscopic investigations of the development of the stria vascularis in the ductus cochlearis of the guinea pig fetus]. Acta Anat (Basel) 124(3-4):159-166.
Wang A, Liang Y, Fridell RA, Probst FJ, Wilcox ER, Touchman JW, Morton CC, Morell RJ, Noben-Trauth K, Camper SA, Friedman TB. 1998. Association of unconventional myosin MYO15 mutations with human nonsyndromic deafness DFNB3. Science 280(5368):1447-1451.
Wangemann P. 2002a. K(+) cycling and its regulation in the cochlea and the vestibular labyrinth. Audiol Neurootol 7(4):199-205.
Wangemann P. 2002b. K+ cycling and the endocochlear potential. Hear Res 165(1-2):1-9.
Wangemann P, Itza EM, Albrecht B, Wu T, Jabba SV, Maganti RJ, Lee JH, Everett LA, Wall SM, Royaux IE, Green ED, Marcus DC. 2004. Loss of KCNJ10 protein expression abolishes endocochlear potential and causes deafness in Pendred syndrome mouse model. BMC Med 2:30.
Wangemann P, Schacht J. 1996. Homeostasic mechanisms in the cochlea. In: Dallos P, Popper, A.N., & Fay, R., editor. Handbook of auditory research: The cochlea. New York: Springer. p 130-185.
Weber PC, Cunningham CD, 3rd, Schulte BA. 2001. Potassium recycling pathways in the human cochlea. Laryngoscope 111(7):1156-1165.
Webster M, Webster DB. 1981. Spiral ganglion neuron loss following organ of Corti loss: a quantitative study. Brain Res 212(1):17-30.
Wehrle-Haller B. 2003. The role of Kit-ligand in melanocyte development and epidermal homeostasis. Pigment Cell Res 16(3):287-296.
Vetter DE, Mann JR, Wangemann P, Liu J, McLaughlin KJ, Lesage F, Marcus DC, Lazdunski M, Heinemann SF, Barhanin J. 1996. Inner ear defects induced by null mutation of the isk gene. Neuron 17(6):1251-1264.
Willems P, editor. 2004. Genetic hearing loss. New York: Marcel. Dekker. 469 p.
Zelante L, Gasparini P, Estivill X, Melchionda S, D'Agruma L, Govea N, Mila M, Monica MD, Lutfi J, Shohat M, Mansfield E, Delgrosso K, Rappaport E, Surrey S, Fortina P. 1997. Connexin26 mutations associated with the most common form of non-syndromic neurosensory autosomal recessive deafness (DFNB1) in Mediterraneans. Hum Mol Genet 6(9):1605-1609.
Zidanic M, Brownell WE. 1990. Fine structure of the intracochlear potential field. I. The silent current. Biophys J 57(6):1253-1268.
Zsebo KM, Williams DA, Geissler EN, Broudy VC, Martin FH, Atkins HL, Hsu RY, Birkett NC, Okino KH, Murdock DC, et al. 1990. Stem cell factor is encoded at the Sl locus of the mouse and is the ligand for the c-kit tyrosine kinase receptor. Cell 63(1):213-224.
Ågrup C, Berggren PO, Köhler M, Spångberg ML, Bagger-Sjöbäck D. 1996. Morphological and functional characteristics of the different cell types in the stria vascularis: a comparison between cells obtained from fresh tissue preparations and cells cultured in vitro. Hear Res 102(1-2):155-166.